JCTC Journal of Chemical Theory and Computation

Article

pubs.acs.org/JCTC

Performance of the EOMIP-CCSD(2) Method for Determining the Structure and Properties of Doublet Radicals: A Benchmark Investigation

Achintya Kumar Dutta, Nayana Vaval, and Sourav Pal*

Physical Chemistry Division, CSIR-National Chemical Laboratory, Pune-411008, India

Supporting Information

ABSTRACT: We present a benchmark study on the performance of the EOMIP-CCSD(2) method for computation of structure and properties of doublet radicals. The EOMIP-CCSD(2) method is a second-order approximation to the standard EOMIP-CCSD method. By retaining the black box nature of the standard EOMIP-CCSD method and adding favorable N^5 scaling, the EOMIP-CCSD(2) method can become the method of choice for predicting the structure and spectroscopic properties of large doublet radicals. The EOMIP-CCSD(2) method overcomes the typical problems associated with the standard single reference ab initio treatment of doublet radicals. We compare our results for geometries and harmonic vibrational frequencies with those obtained using the standard EOMIP-CCSD method, as well as unrestricted Hartree−Fock (UHF)- and restricted open-shell Hartree−Fock (ROHF)-based single-reference coupled-cluster and second order many-body perturbation theory (MBPT(2)) methods. The effect of the basis set on the quality of the results has been studied using a hierarchy of Dunning's correlation-consistent aug-cc-pVXZ (X = D, T, Q) basis sets. Numerical results show that the EOMIP-CCSD(2) method, despite its N^5 scaling, gives better agreement with experimental results, compared to the UHF- and ROHF-based MBPT(2), as well as the single-reference coupled-cluster methods.

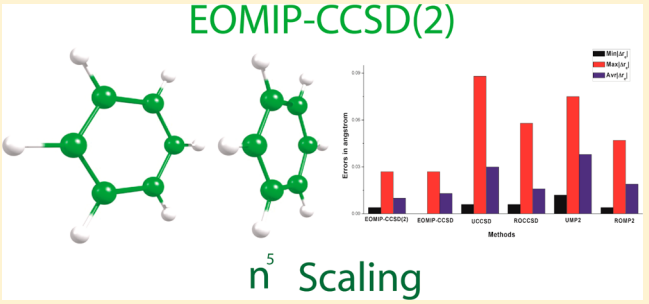

1. INTRODUCTION

In recent times, ab initio quantum chemistry has become the trusted companion of researchers for the elucidation of structures and properties of complicated molecules. Among the plethora of methods available, the single-reference coupled-cluster method,[1,2] because of its systematic treatment of electron correlation, has emerged as the method of choice for accurate prediction of structure,[3−5] properties,[6] and vibrational spectra[7−9] of closed-shell molecules. The extension of the single-reference coupled-cluster method to open-shell systems, based on unrestricted Hartree−Fock (UHF)[10] or restricted open-shell Hartree−Fock (ROHF)[11,12] references, has also been achieved. However, the single-reference coupled-cluster method, even in the singles and doubles approximation, scales as N^6 power with the basis set, whereas the inclusion of partial triples[13−15] (CCSD(T)) increases the scaling to N^7. The development of parallel codes and a rapid increase in computational power, in recent times, may have made coupled-cluster calculations for small- and medium-sized molecules possible (at least in small basis sets). However, the structure and property calculations of medium-sized molecules, in moderately sized or big basis sets, are still not routine. Moreover, N^6 scaling is computationally demanding to use in quantum molecular dynamics calculations, which involves multiple force constant calculations and is essential for predicting the time evolution and temperature effect on the molecules. Thus, a theoretical method with scaling lower than N^6, that is still able to predict the properties of the molecule accurately, is the need of the day.

The standard second order many-body perturbation theory (MBPT(2)) method offers the first correlation correction to the energy over the Hartree−Fock method and scales as N^5 with the basis set. Over the years, the method has been extensively used as an accurate tool for ab initio investigation on a large variety of closed-shell molecules. But, standard UHF-based[16] or ROHF-based[17,18] MBPT(2) methods perform poorly in the case of open-shell doublet radicals, because of multiple problems[19−21] associated with the open-shell single reference wave function, such as spin contamination,[22,23] symmetry breaking,[24] near-singularities of the HF solution,[25,26] pseudo-Jahn−Teller effects,[27] and the presence of multireference character.

However, ab initio investigation of doublet radicals is extremely important, because of the key role of the radicals in biology and chemistry. The high energy and short lifetime of a doublet radical makes experimental characterization often tedious, and sometimes impossible. Theoretical calculations[28−34] can be helpful to understand the doublet radicals and their mechanism in chemistry and biology. However, this is more difficult for open-shell molecules, mainly because of two reasons:

Received: April 18, 2013
Published: August 20, 2013

ACS Publications © 2013 American Chemical Society

(1) The radical wave function has a more-complicated spin structure than that in the closed-shell molecules, in which all electrons are paired.
(2) Two or more configurations make dominant contributions to the reference wave function in the radicals.

The multireference perturbation theory (MRPT) method,[35−38] the multireference configuration interaction (MRCI) method,[39,40] and the multireference coupled-cluster (MRCC) method[41−51] can avoid the above-mentioned problems. However, the results are strongly dependent on the choice of active space, which requires experience and expertise. Subsequently, these calculations cannot be performed with a mere "push of a button".

On the other hand, the equation of motion−coupled-cluster (EOM-CC) method[52−55] incorporates a balanced description of the dynamic and non-dynamic correlation and presents a black box approach for the accurate calculation of energy,[53−58] structure,[59−61] and properties[62] of open-shell molecules and molecular excited states. The EOMIP-CCSD method has been successfully used[63−67] to investigate the structure and properties of problematic doublet radicals. However, despite having otherwise favorable characteristics, the EOMIP−CCSD method still has the problem of N^6 scaling. Stanton and Gauss[68] proposed an N^5-scaled size-extensive modification of the standard EOMIP-CCSD method, by approximating the effective Hamiltonian based on perturbative orders. They have coined the term EOMIP-CCSD(2) for this black box method, and they have shown favorable numerical results for the formyl radical in the DZP basis set. One molecule is too inadequate to make a benchmark and the basis set used was too small to make a definitive conclusion. However, their results were very promising and if the trend generally holds, the EOMIP-CCSD(2) method can become the method of choice for the theoretical treatment of doublet radicals. The objective of this paper is to perform a benchmark EOMIP-CCSD(2) study on the geometry and infrared (IR) spectroscopic properties for a variety of doublet radicals and compare the performance relative to experiment, with those obtained by standard EOM-IP-CCSD, single-reference MBPT(2), and CCSD methods.

The paper is organized as follows. Section 2 gives a brief discussion on the theory of the EOMIP-CCSD(2) method and computational details of the calculations. The trends in the numerical results for the geometry and IR frequency of a set doublet radicals are discussed in section 3. Section 4 contains the conclusions.

2. THEORY AND COMPUTATIONAL DETAILS

The nonvariational coupled-cluster method generates the correlated wave function from a single Slater determinant reference state by the action of an exponential operator.

$$|\psi\rangle = e^T|\phi_0\rangle \tag{1}$$

$|\phi_0\rangle$ is generally, but not necessarily, the Hartree−Fock determinant and $T = T_1 + T_2 + T_3 + \ldots T_n$, where

$$\hat{T}_1 = \sum_{ia} t_i^a\{a_a^\dagger a_i\}$$

$$\hat{T}_2 = \frac{1}{4}\sum_{ijab} t_{ij}^{ab}\{a_a^\dagger a_b^\dagger a_j a_i\}$$

$$\hat{T}_3 = \frac{1}{6}\sum_{ijkabc} t_{ijk}^{abc}\{a_a^\dagger a_b^\dagger a_c^\dagger a_k a_j a_i\} \tag{2}$$

These amplitudes are generally obtained by the iterative solution of a system of coupled nonlinear equations. Extending T up to the nth order, where n equals the total number of electrons in the system, leads to the full CI solution. However, for practical applications, T is truncated to finite order. The exponential structure of the correlation operator ensures the size extensivity, even at the truncated level of T. The truncation of T amplitudes at T_1 and T_2 leads to the popular coupled-cluster singles and doubles (CCSD) approximation, which scales as N^6 with the basis set (where N is the number of basis functions). The inclusion of higher excitations leads to a systematic improvement in accuracy, but at the expense of a substantial increase in computational cost. The CCSDT method[69,70] scales as N^8 and the inclusion of quadruples excitation (CCSDTQ)[71] advances the computational scaling to N^{10}.

The coupled-cluster method shares an intimate relationship with the many-body perturbation theory (MBPT).[72] Suitable lower-order iterations of coupled-cluster equations recover the various orders of MBPT. For example, the lowest-order approximation to the coupled-cluster T_2 amplitudes leads to the standard MBPT(2) method.

The single-reference coupled-cluster method includes dynamic correlations in a systematic way. However, it fails to account for the non-dynamic correlation, which arises due to the quasi-degenerate states that prevail in radicals, bond stretching, and molecular excited states. Consequently, the single-reference coupled-cluster methods, especially in the CCSD approximation, perform poorly in the above-mentioned cases. A multireference coupled-cluster (MRCC) method[41−51] addresses both dynamic and nondynamic correlations in a systematic way. However, it has the active space dependency problem, as discussed previously.

Along with the MRCC methods, the EOM-CC method is known for its balanced treatment of both dynamic and nondynamic correlations. In the EOM-CC method, the final states are obtained by diagonalizing the similarity transformed Hamiltonian

$$\bar{H} = e^{-T}He^T = (He^T)_c \tag{3}$$

The subscript "c" in the above equation represents the connectedness of T with H. Since e^T is not unitary, $\bar{H}$ is not Hermitian. Therefore, the final states are represented by a biorthogonal set of bra and ket vectors, which are parametrized by left and right eigen vectors of $\bar{H}$, denoted by L and R, respectively.

$$\langle\tilde{\Psi}| = \langle\phi_0|Le^{-T} \tag{4}$$

$$|\Psi\rangle = e^T R|\phi_0\rangle \tag{5}$$

For ionization problems, $\langle\tilde{\Psi}|$ and $|\Psi\rangle$ do not correspond to particle conserving operators, but rather involve the net creation (L) and annihilation (R) of one electron. L and R can be expressed in second quantization notation as follows:

$$L \equiv \sum_i l^i i^\dagger + \frac{1}{2}\sum_{ija} l_a^{ij} i^\dagger a j^\dagger \tag{6}$$

$$R \equiv \sum_i r_i i + \frac{1}{2}\sum_{ija} r_{ij}^a a^\dagger i j \tag{7}$$

Diagonalization of $\bar{H}$ in the $(N-1)$ electron space gives the singly ionized states of an N-electron state and the theory is called the EOMIP-CC method. It is equivalent to the (0,1) sector of the

Fock space multireference coupled-cluster (FSMRCC) method for the principal ionizations.[73] FSMRCC has been successfully implemented for spectra,[47,49,51,74−76] properties,[77] and transition moments.[78,79]

The energy, using the EOMIP-CC method, can be written in the following illustrative functional form:

$$E = \langle \phi_0 | L\bar{H}R | \phi_0 \rangle = \langle \phi_0 | Le^{-T}He^{T}R | \phi_0 \rangle \quad (8)$$

The EOMIP-CC method is commonly used in singles and doubles approximation (EOMIP-CCSD). It has the same N^6 scaling as that of the single-reference CCSD method and similar storage requirements, which prohibit its applications beyond the first-row atoms, in a moderate basis set. Thus, it is highly desirable to develop methods, similar in spirit to the standard EOMIP-CCSD but with lower computational scaling and smaller storage requirements. Nooijen and Snijders[80] were the first to propose a simplification[81,82] to the standard EOM-IP-CCSD method, by approximating the full CCSD similarity transformed Hamiltonian as

$$\bar{H} \equiv \bar{H}_{\mathrm{NS}} = e^{-T^{[1]}}He^{-T^{[1]}} \quad (9)$$

$\bar{H}_{\mathrm{NS}}$ is complete up to the first order in correlation and contains selective contributions from higher-order terms. Diagonalization of $\bar{H}_{\mathrm{NS}}$ in the $(N-1)$ electron space leads to the loss of size extensivity in energy. Nooijen and Snijders had eliminated the problem by diagonalizing matrix elements of a modified operator A, in place of $\bar{H}_{\mathrm{NS}}$, where

$$A_{\mu\nu} = \langle \phi_0 | \Omega_\mu [\bar{H}_{\mathrm{NS}}, \Omega_\nu^\dagger] | \phi_0 \rangle \quad (10)$$

$\Omega^\dagger = \{a_i; a_i a_a^\dagger a_j\}$, and it represents the elements of the set of creation operator string that maps the $|\phi_0\rangle$ into the determinants spanning the diagonalization space. The commutator in the equation accounts for all of the missing second-order contributions to $\bar{H}_{\mathrm{NS}}$, whereas third- or higher-order terms in A do not contribute to the truncated diagonalization problem. This ensures the size extensivity in energy. However, the method does not provide a clear definition for the total energy and, thus, becomes unsuitable for studying properties of the final state.

Stanton and Gauss provided an alternative approach for approximating the conventional EOM-CCSD method.[68] They have expanded the effective Hamiltonian in a perturbation series:

$$\bar{H} = (He^{T})_c = \bar{H}^{[1]} + \bar{H}^{[2]} + \bar{H}^{[3]} + \ldots \bar{H}^{[n]} \quad (11)$$

The bracketed superscript in the above equation represents the order in perturbation and subscript c represents the connectedness of T with H. This leads to a set of hierarchical approximations to the full $\bar{H}$, and the diagonal representation of the modified effective Hamiltonian offers a set of hierarchical approximations to the corresponding EOM-CC final states, known as EOMCCSD(n). At large values of n, $\bar{H}^{[n]}$ converges to the full $\bar{H}$ and, consequently, EOMCCSD(n) converges to the standard EOM-CCSD. The approximate similarity transformed Hamiltonian, truncated at the nth order, includes only the terms up to the order n in perturbation, which ensures the size extensivity of the final energy for all values of n. Truncation at $n = 2$, leads to EOMCCSD(2), with a MBPT(1) ground-state reference wave function and a MBPT(2) ground-state energy. The EOMCCSD(2) method provides an energy difference value that is identical to that of the Nooijen and Snijders's method and has the additional advantage of a clearly defined final energy.

The diagonalization of $H^{[2]}$ in a space spanned by a subset of $(N-1)$ determinants leads to the final ionized states of N-electron molecular problem, which can be performed by slight modification of any standard EOMIP-CCSD code. The explicit derivation of the expressions has been presented in ref 68. The EOMIP-CCSD(2)method is naturally spin-adapted and equipped to deal with multireference situations, and, therefore, it is free from the problems that are associated with the standard single-reference treatment for doublet radicals.

The truncation of the effective Hamiltonian, based on perturbation order, leads to an obvious loss in accuracy. However, it gains significant computational simplifications, which lead to advantages in terms of both CPU timing and storage. The computational requirements of the standard EOMIP-CCSD method are dominated by the N-electron reference state CCSD calculation. Approximating the reference state using the MBPT(1) wave function reduces the computational scaling of the reference state calculation to N^5, as opposed to the iterative N^6 scaling of the CCSD reference-state calculation. Now, in IP calculation, the diagonalization (using Davidson's iterative method) of the $\bar{H}$ scales as N^5 and the superficially N^6 scaling intermediates can also be computed in an iterative N^5 scaling algorithm, by calculating them on the fly.[83] Thus, overall, the EOMIP−CCSD(2) method scales as N^5, which is vastly more economical[84,85] than the standard EOMIP-CCSD method.

The terms containing the $(ab|cd)$-type integral present the most computationally demanding part of the coupled-cluster iterations. The large file size of the four particle integrals often becomes the limiting factor for storage and memory. It also slows the overall speed of the calculation, by creating input/output (I/O) bottlenecks, even for small molecules. Now, $(ab|cd)$ integrals only contribute to the reference-state CCSD calculation and, consequently, remain totally absent in the EOM part for the ionization problem. Thus, approximating the reference-state wave function at MBPT(1) leads to a significant savings in terms of disk space, since it does not require the $(ab|cd)$ integrals. The favorable N^5 scaling and reduced storage requirements[86] make the EOMIP-CCSD(2) method applicable to the systems of considerably large dimension, where the use of the normal EOMIP-CCSD method is not possible.

T1 diagnosis values presented in the paper are calculated using Gaussian 09.[87] All the other results presented in the paper are calculated using CFOUR.[88] All of the electrons are used in the correlation calculations. Dunning's correlation-consistent aug-cc-pVXZ (X = D, T, Q) basis sets[89] are used in the calculations. Equilibrium geometries (r_e) without any vibrational averaging and harmonic vibrational frequencies are used for comparison with the experiments.

3. RESULTS AND DISCUSSIONS

To compare the timing of EOMIP-CCSD(2) with standard EOMIP-CCSD, we have calculated the ionization potential of water clusters($(H_2O)_n$, where $n = 1-8$) in cc-pVDZ basis set. The wall timings are presented in Table 1. The EOMIP-CCSD(2) method is found to be computationally significantly less expensive than the EOMIP-CCSD method.

To benchmark the reliability of the EOMIP-CCSD(2) method, we have calculated the geometry and vibrational frequencies of NO_2, NO_3, trans ONOO, NO, CN, F_2^+, CO^+, O_2^+, and N_2^+ in aug-cc-pVDZ, aug-cc-pVTZ, and aug-cc-pVQZ basis. The above-mentioned radicals present a significant challenge for conventional ab initio methods. In all of the cases, the results are compared with those obtained by standard

Table 1. Wall Timings for the EOMIP-CCSD(2) and EOMIP-CCSD Method[a,b] in the cc-pVDZ Basis Set

number of H_2O units	Wall Timing (s)	
	EOMIP-CCSD	EOMIP-CCSD(2)
1	1.42	1.40
2	5.30	2.30
3	20.22	4.77
4	83.64	14.63
5	236.00	39.86
6	550.86	81.69
7	1385.21	223.21
8	3964.00	700.91

[a]All the calculations were performed using an i7 desktop with 3.40 GHz CPU speed and 16 GB of RAM. Calculations were performed using single core. [b]Calculations were performed assuming C_1 symmetry.

EOMIP-CCSD, UMP2, ROMP2, UCCSD, and ROCCSD methods, as well as with available experimental data. To test the suitability of the EOMIP-CCSD(2) method for larger radicals, the geometry and IR frequencies have been calculated for the water dimer cation, the formate radical, the uracil cation, the acetylene dimer cation, and the benzene dimer cation as test cases, and the results are compared with those obtained using the standard EOMIP-CCSD method.

A. Nitrogen Dioxide (NO_2). Nitrogen dioxide (NO_2) is a very important molecule in atmospheric chemistry; consequently, it is subjected to many computational investigations.[63,90−92] The triplet instabilities and second-order Jahn−Teller (SOJT) effect in NO_2, lead to the mixing of $^2A_1$ and $^2B_2$ states, which makes the description of vibrational modes—especially the asymmetric stretching problematic. The T1 diagnosis value of 0.026 (Table 2)

Table 2. T1 Diagnosis Value of the Doublet Radicals

molecule	T1 diagnosis
NO	0.023
CN	0.050
F_2^+	0.013
CO^+	0.046
O_2^+	0.014
N_2^+	0.022
NO_2	0.026
NO_3	0.035
ONOO	0.034

indicates significant multireference character of the molecule. Table 3 presents the geometry and the vibrational frequencies for NO_2.

In the aug-cc-pVDZ basis set, the EOMIP-CCSD(2) method shows excellent agreement with the experiment for both bond lengths ($|\Delta r_e|$ = 0.006 Å) and bond angles ($|\Delta_{angle}|$ = 0.3°). The method also provides very good agreement with the experiment[93,94] for the bending mode of vibration ($|\Delta\omega_e|$ = 6 cm^{-1}). However, it overestimates both symmetric stretching modes (($|\Delta\omega_e|$ = 45 cm^{-1}) and asymmetric stretching modes ($|\Delta\omega_e|$ = 120 cm^{-1}), which are consistent with the previous theoretical reports.[61,88] The performance of the EOMIP-CCSD method is similar to that of the EOMIP-CCSD(2) method, for both bond lengths ($|\Delta r_e|$ = 0.007 Å) and bond angles ($|\Delta_{angle}|$ = 0.6°). The asymmetric stretching ($|\Delta\omega_e|$ = 85 cm^{-1}) mode is comparatively

Table 3. Geometry and Harmonic Vibrational Frequency of Nitrogen Dioxide (NO_2)

method	bond length (Å)	bond angle (θ)	ω_1 (cm^{-1})	ω_2 (cm^{-1})	ω_3 (cm^{-1})
aug-cc-pVDZ Basis Set					
EOMIP-CCSD(2)	1.2000	134.2	756	1370	1754
EOMIP-CCSD	1.201	133.3	772	1413	1719
UCCSD	1.299	124.51	577	955	908*i*
ROCCSD	1.197	134.7	767	1412	1721
UMP2	1.284	125.0	671	1138	1629
ROMP2	1.216	132.6	753	1317	1844
aug-cc-pVTZ Basis Set					
EOMIP-CCSD(2)	1.186	134.9	769	1384	1784
EOMIP-CCSD	1.186	133.7	795	1425	1745
UCCSD	1.283	124.9	139*i*	596	1190
ROCCSD	1.181	135.2	785	1438	1762
UMP2	1.270	125.4	609	1273	1071*i*
ROMP2	1.201	133.2	763	1329	1844
aug-cc-pVQZ Basis Set					
EOMIP-CCSD2	1.185	135.7	773	1391	1782
EOMIP-CCSD	1.185	133.4	802	1450	1744
UCCSD	1.282	124.8	169*i*	603	1199
ROCCSD	1.180	135.0	790	1443	1762
UMP2	1.269	125.23	614	1279	1073*i*
ROMP2	1.200	133.0	767	1331	1840
Experimental Results					
	1.194[a]	133.9[a]	750[b]	1325[b]	1634[b]

[a]Values taken from ref 93. [b]Values taken from ref 94.

well-described in the EOMIP-CCSD method. However, it shows more error than the EOMIP-CCSD(2) method for the bending mode ($|\Delta\omega_e|$ = 22 cm^{-1}), as well as symmetric stretching mode ($|\Delta\omega_e|$ = 88 cm^{-1}). The UCCSD method performs very poorly for both geometry and vibrational frequencies; it especially underestimates the asymmetric stretching mode by a large value of 726 cm^{-1}. This is due to instabilities associated with the unrestricted reference wave function, which is indicated by a negative eigen value of the orbital rotation Hessian. The same reason leads to the disastrous performance of the UMP2 method. The performance of the ROCCSD method is similar to that of the EOMIP-CCSD method, with regard to geometry and harmonic vibrational frequencies. The ROMP2 method, on the other hand, shows more error than the EOM and ROCCSD methods for bond length ($|\Delta r_e|$ = 0.022 Å) and bond angle ($|\Delta_{angle}|$ = 1.3°), but performs significantly better than both the UCCSD and UMP2 methods. The ROMP2 method performs surprisingly well for bending and symmetric stretching modes of vibration. However, it significantly overestimates the asymmetric stretching mode ($|\Delta\omega_e|$ = 210 cm^{-1}).

Upon moving from the aug-cc-pVDZ basis set to the aug-cc-pVTZ basis set, the bond length shrinks and the bond angles are stretched for all of the theoretical methods. The EOMIP-CCSD(2) method continues to give a similar performance to that of the EOMIP-CCSD method, with regard to geometry, but gives better agreement with the experiment in the case of harmonic vibration frequencies. However, both methods overestimate the experimental asymmetric stretching frequency. The UCCSD method continues to give poor performance, with regard to geometry and harmonic vibrational frequencies. The imaginary value of the bending mode indicates that the optimized geometry in the UCCSD method is not actually the minimum on the potential energy surface, but rather is a first-order saddle point. The ROCCSD method avoids the disastrous failure of the

dx.doi.org/10.1021/ct400316m | J. Chem. Theory Comput. 2013, 9, 4313−4331

Table 4. Geometry and Harmonic Vibrational Frequency of Nitrogen Trioxide (NO_3)

	Bond Length (Å)		Vibrational Frequency (cm^{-1})					
method	L_1	L_2	ω_1 (asym bend)	ω_2 (asym bend)	ω_3 (umbrella)	ω_4 (sym stretch)	ω_5 (asym stretch)	ω_6 (asym stretch)
augcc-pVDZ Basis Set								
EOMIP-CCSD(2)	1.240	1.240	163	163	783	1130	1198	1198
EOMIP-CCSD	1.235	1.235	310	310	813	1149	1183	1183
UCCSD	1.261	1.197	528	630	810	1129	1102	1667
ROCCSD	1.261	1.198	7792*i*	520	785	1116	1647	277833
UMP2	1.284	1.204	682	702	667	1058	791i	1650
ROMP2	1.267	1.220	521	655	833	1087	1642	2097
aug-cc-pVTZ Basis Set								
EOMIP-CCSD(2)	1.228	1.228	66	66	800	1140	1176	1176
EOMIP-CCSD	1.221	1.221	305	305	836	1170	1191	1191
UCCSD	1.247	1.182	552*i*	857	826	1174	581	1700
ROCCSD	1.247	1.183	538	619	807	1139	998	1778
UMP2	1.270	1.191	701	908*i*	615	1081	716	1648
ROMP2	1.255	1.206	526	663	842	1097	1643	2123
aug-cc-pVQZ Basis Set								
EOMIP-CCSD(2)	1.227	1.227	95	95	801	1142	1175	1175
EOMIP-CCSD	1.219	1.219	314	314	838	1174	1192	1192
UCCSD	1.246	1.182	547	7917	779	1152	1693	27249*i*
ROCCSD	1.246	1.182	442	623	809	1143	1005	1682
UMP2	1.269	1.190	703	910*i*	612	1085	718	1650
ROMP2	1.254	1.205	526	664	843	1099	1644	2126
Experimental Results								
	1.240[a]	1.240[a]	250[b]	250[b]	762[c]	1060[c]	1480[c]	1480[c]

[a]Values taken from ref 98. [b]Values taken from ref 95. [c]Values taken from ref 96.

UCCSD method, but gives inferior performance, compared to the EOM methods. The UMP2 method suffers from the spin contamination problem, similar to that of the UCCSD method; consequently, the results show a large deviation from the experimental bond length and bond angle. The asymmetric stretching mode in the UMP2 method shows an imaginary value, indicating that the geometry is a first-order saddle point. The ROMP2 method gives remarkable agreement with the experimental values with regard to geometry, as well as bending and stretching modes of vibration, but it overestimates the asymmetric stretching mode of vibration, and shows greater error ($|\Delta\omega_e| = 204\ cm^{-1}$) than the EOM-based methods.

The same trend persists in the aug-cc-pVQZ method, where the geometries and IR frequencies for all of the methods show very little deviation from their corresponding values in the aug-cc-pVTZ basis set.

B. Nitrogen Trioxide (NO_3). The ground-state geometry of the nitrogen trioxide (NO_3) radical has been an issue of long-standing debate. Experimental studies[95−99] have provided evidence in favor of D_{3h} geometry, whereas various theoretical studies have predicted different minimum energy structures for the molecule. Three structures have been found to be energetically most favorable: (a) a highly symmetric D_{3h} structure, (b) a C_{2v} structure with two long bonds and one short bond (2L1S), and (c) C_{2v} structure with one long bond and two short bonds (1L2S). Initial MCSCF studies[100] have predicted a Y-shaped structure for the NO_3 radical. In 1992, Bartlett and co-workers[101] have reported the C_{2v} structure to be 2.5 kcal/mol lower in energy than the more-symmetric D_{3h} structure in the B-CCD level of theory. Crawford and Stanton[102] latter revised this ordering, by placing the D_{3h} structure 0.5 kcal/mol below the C_{2v} structure in the B-CCD(T) method. The T1 diagnosis value of 0.035 (Table 2) indicates significant multireference character for the species. Fock space multireference coupled-cluster (FSMRCC) calculations by Kaldor,[103] and MRCI calculations by Morkuma and Eisfield,[104] both resulted in a D_{3h} ground-state geometry for the NO_3 radical.

The EOMIP-CCSD(2) and EOMIP-CCSD methods predict a D_{3h} ground-state geometry. In the aug-cc-pVDZ basis set, the EOMIP-CCSD(2) method shows better agreement with the experimental bond length than the EOMIP-CCSD method. Both methods slightly underestimate the bond length in the aug-cc-pVTZ and aug-cc-pVQZ basis sets. However, the EOMIP-CCSD(2) method continues to give better agreement with the experiment than the EOMIP-CCSD method. The UCCSD and ROCCSD methods predict a C_{2v} minimum energy structure (2L1S) for the ground state and both the methods predict identical geometries. In the aug-cc-pVDZ basis set, both methods overestimate the experimental bond length, in the case of the long bonds (2L) and underestimate the experimental bond length in the case of the short bond (1S). The two long bonds shrink in the aug-cc-pVTZ and aug-cc-pVQZ basis sets, bringing them closer to the experimental value. However, the use of a large basis set also shrinks the shorter bond, taking it further away from the experimental value. The UMP2 and ROMP2 methods follow the trend of their coupled-cluster analogues, only with a larger error bar.

The EOMIP-CCSD(2) method performs reasonably well for the IR frequencies of NO_3. It predicts the umbrella (ω_3) and the symmetric stretching (ω_4) mode of vibrations with high accuracy. However, it underestimates the low-frequency asymmetric bending (ω_1 and ω_2) and high-frequency asymmetric stretching (ω_5 and ω_6) modes (see Table 4). The umbrella and symmetric stretching modes shift to higher values, when using larger basis sets; whereas, all of the other modes of vibration shrink to lower values. While the EOMIP-CCSD method shows significant improvement over the EOMIP-CCSD(2) method, for the asymmetric bending mode, it reduces

dx.doi.org/10.1021/ct400316m | J. Chem. Theory Comput. 2013, 9, 4313−4331

Table 5. Geometry and Harmonic Vibrational Frequency of Trans Nitro Peroxide (OONO)

	Bond Length (Å)			Bond Angle (deg)		Vibrational Frequency (cm^{-1})					
method	O−O	N−O	O−N	N−O−O	O−N−O	ω_1	ω_2	ω_3	ω_4	ω_5	ω_6
aug-cc-pVDZ Basis Set											
EOMIP-CCSD(2)	1.285	1.557	1.157	109.5	108.1	193	361	452	881	1287	1800
EOMIP-CCSD	1.298	1.598	1.149	106.6	108.2	150	351	421	848	1207	1902
UCCSD	1.216	3.316	1.159	88.3	166.1	61i	33	36	36	1581	1946
ROCCSD	1.352	1.605	1.143	110.1	108.3	192	260	368	701	929	1900
UMP2	1.259	3.146	1.141	73.4	171.0	8	58	65	170	1219	3658
ROMP2	1.328	1.762	1.137	110.9	108.7	170	226	310	675	913	1980
aug-cc-pVTZ Basis Set											
EOMIP-CCSD(2)	1.275	1.537	1.144	110.1	108.2	199	366	468	901	1307	1815
EOMIP-CCSD	1.287	1.556	1.136	107.4	108.3	158	368	450	870	1251	1925
UCCSD	1.196	3.224	1.142	79.3	169.2	102*i*	79	181	277	1646	1957
ROCCSD	1.281	1.582	1.136	107.8	108.2	181	280	338	723	1170	1867
UMP2	1.243	3.034	1.135	78.2	186.1	50	40	79	441	1329	3139
ROMP2	1.229	1.183	1.136	107.8	110.2	1916*i*	113	105	522	1055	1805
aug-cc-pVQZ Basis Set[b]											
EOMIP-CCSD(2)	1.274	1.540	1.143	110.2	108.3	198	364	465	897	1307	1811
EOMIP-CCSD	1.287	1.557	1.135	107.5	108.3	157	368	451	870	1250	1919
UCCSD	1.196	3.332	1.141	79.6	169.6	17	34	43	53	1673	2000
ROCCSD	1.337	1.564	1.129	111.1	108.6	200	272	393	731	989	1912
UMP2	1.226	3.229	1.135	79.1	169.1	9*i*	41	50	63	1428	3169
ROMP2	1.227	1.849	1.136	108.2	110.2	117	197	202	700	1336	1924
Experimental Results											
											1840[a]

[a]Value taken from ref 107. [b]Diffused *g* functions were excluded from the basis to keep the calculations computationally viable.

the accuracy of the umbrella and symmetric stretching modes. Both EOMIP-CCSD(2) and EOMIP-CCSD methods, however, significantly underestimate the asymmetric stretching mode. Here, it should be noted that the experimental assignments of the asymmetric stretching at 1492 cm^{-1} is not unambiguous.[64] Detailed studies are required to make a concluding statement about these problematic modes, which are beyond the scope of the present study. The single-reference coupled-cluster methods show large errors for the harmonic vibrational frequencies. The UCCSD method, in aug-cc-pVDZ basis, overestimates the two asymmetric bending modes and one of the asymmetric stretching modes, while it underestimates the other asymmetric stretching mode. These trends continue in the aug-cc-pVTZ basis, where the ω_1 shows an imaginary frequency, indicating that the geometry is a first-order saddle point. The UCCSD method in the aug-cc-pVQZ basis set shows a unphysical value for one of the asymmetric stretching modes (ω_2) and one of the asymmetric bending modes (ω_6) of vibration. The instability in the UHF reference wave function, indicated by the negative eigen value of the orbital rotation Hessian, leads to the catastrophic failure of the UCCSD method in the present case. The UMP2 method follows the same trend as that of its coupled-cluster analogue and shows one imaginary frequency in all of the basis sets. The ROCCSD method shows an imaginary frequency for the asymmetric bending mode (ω_1) in the aug-cc-pVDZ basis set, indicating that the geometry is a first-order saddle point. It also gives an unphysical value for the asymmetric stretching mode (ω_6). Although these spurious results vanish at higher aug-cc-pVTZ and aug-cc-pVQZ basis sets, the calculated IR frequencies still show large deviations from the experimental results. The ROMP2 method closely follows the trend of ROCCSD method, with the difference being that the former does not show any unphysical or imaginary frequencies in any of the basis sets used.

C. Trans Nitro Peroxide (OONO). The correlation of experiments and theory for the trans nitro peroxide has been a matter of long-standing debate.[105,106] Bhatia and Hall[109] have suggested a planar trans structure from IR spectroscopic investigation. However, later ab initio studies,[105,108,109] using different levels of theories, have shown contradictory results. The radical shows considerable multireference character (T1 diagnosis value = 0.034), making it a challenging case for standard ab initio methods. Geometry and IR frequencies of trans ONOO, computed at different levels of theory, are presented in Table 5.

The EOMIP-CCSD(2) method shows an O−N bond length of 1.157 Å in the aug-cc-pVDZ basis set. The O−O bond length (1.285 Å) shows considerable elongation from the bare molecular oxygen bond length of 1.207 Å and, consequently, the N−O bond length (1.157 Å) decreases from the free nitric oxide bond length value of 1.160 Å. It indicates an electron transfer from the antibonding orbital of nitric oxide to the antibonding orbital of oxygen, leading to shrinkage of the former and stretching of the latter. In the EOMIP-CCSD(2) method, the IR frequency corresponding to the N−O bond stretching mode (ω_6) is underestimated by 40 cm^{-1}. The EOMIP-CCSD method predicts longer O−O and O−N bond lengths, compared to the EOMIP-CCSD(2) method. On the other hand, the N−O bond shrinks, from 1.157 Å to 1.149 Å, upon moving from the EOMIP-CCSD(2) method to the EOMIP-CCSD method, which leads to overestimation of experimental frequency (62 cm^{-1}) in the latter. The ROCCSD and ROMP2 methods follow the same trend as that of the EOMIP-CCSD method. However, the UCCSD method predicts a weakly bound T-shaped geometry (Figure 1) with an elongated O−N bond length of 3.316 Å. The O−O and the N−O bond lengths are almost same as that of their free molecular form. The structure shows an imaginary frequency, which indicates that the geometry is a

dx.doi.org/10.1021/ct400316m | J. Chem. Theory Comput. 2013, 9, 4313−4331

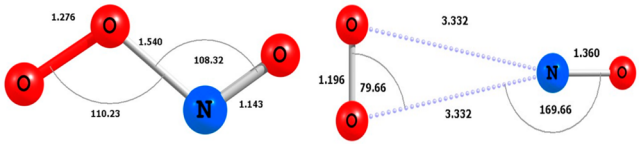

Figure 1. EOMIP-CCSD(2) and UCCSD optimized structure of trans nitro peroxide (ONOO) in the aug-cc-pVQZ basis set.

saddle point of order one. The IR frequency corresponding to the ω_6 mode shows a value of 1946 cm^{-1}, which is 106 cm^{-1} higher than the experimental value. The UMP2 method also shows a T-shaped structure, but with a larger O−O bond, and a shorter O−N bond, as well as a shorter N−O bond. The UMP2 method predicts an N−O bond stretching frequency of 3658 cm^{-1}, which is almost double the experimental frequency of 1840 cm^{-1}. The UHF instability, which is indicated by the negative value of the orbital rotation Hessian, is responsible for the unphysical behavior of the N−O stretching in the UMP2 method.

The EOM methods, as well as the UCCSD method, lead to shrinkage of all of the bonds and an upward shifting of the IR frequencies in the aug-cc-pVTZ basis set. The ROCCSD and ROMP2 methods show similar trends for the bond length, but the IR frequency corresponding to the ω_6 mode undergoes a downward shift in both methods. The UMP2 method also shows a large downward shift of the ω_6 mode, but still overestimates the experimental frequency by more than a thousand wavenumbers.

The results in the EOMIP-CCSD(2) and EOMCCSD methods in the aug-cc-pVQZ basis set show very small deviations from those in the aug-cc-pVTZ basis set. The EOMIP-CCSD(2) method gives the best agreement ($|\Delta\omega_e|$ = 29 cm^{-1}) with the experimental frequency, among all the methods used. However, the UCCSD and UMP2 methods result in a longer O−N bond in the aug-cc-pVQZ basis set. It is interesting to note that both the N−O bond length and the N−O stretching frequency in the UCCSD and UMP2 methods are very similar to that in the free nitric oxide. It indicates that trans ONOO is a very weakly bound complex, contrary to the stable structure predicted by the EOM methods. In the aug-cc-pVQZ basis set, the ROCCSD method shows shrinkage of the N−O bond, which is reflected in the upward shift of the ω_6 mode. The ROMP2 method also results in an upward shift of the N−O stretching frequencies in the aug-cc-pVQZ basis set, but the N−O bond length remains unchanged from that in the aug-cc-pVTZ basis set.

D. The Diatomics. We have tested the performance of EOMIP-CCSD(2) method for diatomic molecules such as NO, CO^+, CN, F_2^+, O_2^+, and N_2^+. These diatomic molecules suffer from the notorious symmetry breaking problem and often represent a classic challenge for standard single-reference theories.

Nitric oxide acts as a catalyst for the ozone depletion reactions and plays a key role in stratospheric ozone chemistry. Table 6 contains the computed bond length and IR frequency of nitric oxide. In the aug-cc-pVDZ basis set, all the methods overestimate the N−O bond length, compared to the experimental value. The IR frequency in all of the methods shows reasonable agreement with the experiment, except in the UMP2 method, where the experimental frequency is overestimated by 1742 cm^{-1}. The bond length shrinks and, consequently, the IR frequency shifts to a higher value in both the aug-cc-pVTZ and aug-cc-pVQZ basis sets. The EOMIP-CCSD(2) method underestimates the experimental bond length, but gives better agreement compared to the ROCCSD and UCCSD methods. For IR frequencies also, it gives a value ($|\Delta\omega_e|$ = 118 cm^{-1}) comparable to the

Table 6. Geometry and Harmonic Vibrational Frequency of Nitric Oxide

method	bond length (Å)	frequency, ω (cm^{-1})
aug-cc-pVDZ Basis Set		
EOMIP-CCSD(2)	1.160	1981
EOMIP-CCSD	1.164	1957
UCCSD	1.160	1941
ROCCSD	1.159	1958
UMP2	1.142	3646
ROMP2	1.170	1897
aug-cc-pVTZ Basis Set		
EOMIP-CCSD(2)	1.146	2014
EOMIP-CCSD	1.150	1996
UCCSD	1.142	2000
ROCCSD	1.142	2000
UMP2	1.135	3179
ROMP2	1.154	1920
aug-cc-pVQZ Basis Set		
EOMIP-CCSD(2)	1.145	2022
EOMIP-CCSD	1.150	2005
UCCSD	1.141	2012
ROCCSD	1.141	2005
UMP2	1.341	3166
ROMP2	1.154	1922
Experimental Results		
	1.150[a]	1904[a]

[a]Values taken from Huber and Herzberg.[110]

EOMIP-CCSD ($|\Delta\omega_e|$ = 101 cm^{-1}), UCCSD ($|\Delta\omega_e|$ = 112 cm^{-1}), and ROCCSD ($|\Delta\omega_e|$ = 101 cm^{-1}) values, in the aug-cc-pVQZ basis set. The UMP2 method performs very poorly, with regard to bond length ($|\Delta r_e|$ = 0.019 Å) and IR frequency ($|\Delta\omega_e|$ = 1262 cm^{-1}). The ROMP2 method, on the other hand, shows surprisingly close agreement with the experiment,[110] with regard to bond length and IR frequency.

N_2^+ shows a T1 diagnostic value of 0.022 (Table 2); therefore, single-reference methods can treat it with reasonable accuracy. Table 7 shows that, in the aug-cc-pVDZ basis set, the EOMIP-CCSD method shows the best agreement with the experiment, with regard to bond length, but overestimates the experimental IR frequency by more than a hundred wavenumbers. The EOMIP-CCSD(2) method, on the other hand, overestimates the bond length but reproduces the experimental[110] IR frequency ($|\Delta\omega_e|$ = 5 cm^{-1}) with high accuracy. The UHF- and ROHF-based single-reference coupled-cluster methods give similar accuracy as that of the EOMIP-CCSD(2) method for bond length, but lead to greater error in IR frequency. Calculations in the aug-cc-pVTZ basis set result in shrinkage of the bond length and an upward shift of vibrational frequency. The results in the aug-cc-pVQZ basis set show negligible deviation from that in the aug-cc-pVTZ basis. The EOMIP-CCSD(2) method shows the best agreement with experiment for both bond length ($|\Delta r_e|$ = 0.004 Å) and IR frequency ($|\Delta\omega_e|$ = 42 cm^{-1}). The UCCSD and ROCCSD methods underestimate the bond length and consequently overestimate the IR frequency, by 94 and 101 cm^{-1}, respectively. The MBPT(2) methods overestimate the bond length and significantly underestimate the IR frequency. N_2^+ shows two significant exceptions to the trend shown by the previously discussed molecules. First, the UMP2 method performs better than the ROMP2 method; second, the EOMIP-CCSD method performs poorly for both bond length ($|\Delta r_e|$ = 0.010 Å) and IR frequency ($|\Delta\omega_e|$ = 152 cm^{-1}).

dx.doi.org/10.1021/ct400316m | J. Chem. Theory Comput. 2013, 9, 4313−4331

Table 7. Geometry and Harmonic Vibrational Frequency of N_2^+

method	bond length (Å)	frequency, ω (cm^{-1})
	aug-cc-pVDZ Basis Set	
EOMIP-CCSD(2)	1.132	2212
EOMIP-CCSD	1.125	2316
UCCSD	1.130	2245
ROCCSD	1.129	2253
UMP2	1.148	2078
ROMP2	1.155	2008
	aug-cc-pVTZ Basis Set	
EOMIP-CCSD(2)	1.113	2250
EOMIP-CCSD	1.106	2359
UCCSD	1.110	2299
ROCCSD	1.109	2306
UMP2	1.127	2124
ROMP2	1.135	2055
	aug-cc-pVQZ Basis Set	
EOMIP-CCSD(2)	1.112	2249
EOMIP-CCSD	1.104	2359
UCCSD	1.108	2301
ROCCSD	1.107	2308
UMP2	1.126	2123
ROMP2	1.134	2054
	Experimental Results	
	1.116[a]	2207[a]

[a]Values taken from Huber and Herzberg.[110]

O_2^+ shows a very small T1 diagnosis value of 0.014, which indicates that a single determinant reference will be sufficient for the accurate description of the wave function. Table 8 shows that, in the aug-cc-pVDZ basis set, the EOMIP-CCSD(2) method exhibits greater error for the bond length ($|\Delta r_e|$ = 0.011 Å), compared to the EOMIP-CCSD and single-reference coupled-cluster methods, but performs significantly better than both the UMP2 method ($|\Delta r_e|$ = 0.049 Å) and the ROMP2 method ($|\Delta r_e|$ = 0.062 Å). However, the EOMIP-CCSD(2) method gives excellent agreement with the experimental value for IR frequency. The aug-cc-pVDZ basis set, however, is inadequate to rely upon. Calculations in the aug-cc-pVTZ and aug-cc-pVQZ basis sets lead to the contraction of the bond length and increment of the IR frequency, in all of the methods used. In the aug-cc-pVQZ basis set, the EOMIP-CCSD(2) method shows the best agreement with the experiment[110] for both bond length ($|\Delta r_e|$ = 0.004 Å) and harmonic vibrational frequency ($|\Delta\omega_e|$ = 37 cm^{-1}). The EOMIP-CCSD method gives comparable performance for bond length ($|\Delta r_e|$ = 0.009 Å), but performs poorly for IR frequency ($|\Delta\omega_e|$ = 117 cm^{-1}). The single-reference coupled-cluster methods also show inferior results for both bond length ($|\Delta r_e|$ = 0.013 and 0.012 Å for the UCCSD and ROCCSD methods, respectively) and harmonic vibrational frequency ($|\Delta\omega_e|$ = 157 and 162 cm^{-1} for the UCCSD and ROCCSD methods, respectively). The UMP2 method performs very poorly with regard to bond length ($|\Delta r_e|$ = 0.030 Å) and IR frequency ($|\Delta\omega_e|$ = 362 cm^{-1}). However, the predicted values are better than those in the ROMP2 method ($|\Delta r_e|$ = 0.041 Å and $|\Delta\omega_e|$ = 476 cm^{-1}). O_2^+ follows the unique trend shown by MBPT(2) and the EOMIP-CCSD method in N_2^+, as discussed in the previous paragraph.

Table 8. Geometry and Harmonic Vibrational Frequency of O_2^+

method	bond length (Å)	frequency, ω (cm^{-1})
	aug-cc-pVDZ Basis Set	
EOMIP-CCSD(2)	1.127	1908
EOMIP-CCSD	1.123	1981
UCCSD	1.120	2016
ROCCSD	1.119	2022
UMP2	1.166	1457
ROMP2	1.179	1326
	aug-cc-pVTZ Basis Set	
EOMIP-CCSD(2)	1.114	1931
EOMIP-CCSD	1.109	2009
UCCSD	1.105	2049
ROCCSD	1.105	2054
UMP2	1.149	1526
ROMP2	1.160	1410
	aug-cc-pVQZ Basis Set	
EOMIP-CCSD(2)	1.112	1942
EOMIP-CC	1.107	2022
UCCSD	1.103	2062
ROCCSD	1.102	2067
UMP2	1.146	1543
ROMP2	1.157	1429
	Experimental Results	
	1.116[a]	1905[a]

[a]Values taken from Huber and Herzberg.[110]

The T1 diagnosis value (0.050) indicates significant multi-reference character of the CN radical. Table 9 lists the computed bond lengths and IR frequencies of the CN radical. In the aug-cc-pVDZ basis set, however, both EOM methods give disastrous performance for bond length and IR frequency.

Table 9. Geometry and Harmonic Vibrational Frequency of CN

method	bond length (Å)	frequency, ω (cm^{-1})
	aug-cc-pVDZ Basis Set	
EOMIP-CCSD(2)	1.248	1805
EOMIP-CCSD	1.241	1877
UCCSD	1.183	2117
ROCCSD	1.185	2104
UMP2	1.138	2843
ROMP2	1.211	1753
	aug-cc-pVTZ Basis Set	
EOMIP-CCSD(2)	1.165	2137
EOMIP-CCSD	1.163	2178
UCCSD	1.162	2187
ROCCSD	1.163	2167
UMP2	1.123	2916
ROMP2	1.186	1849
	aug-cc-pVQZ Basis Set	
EOM-IP-CCSD(2)	1.164	2133
EOMIP-CCSD	1.161	2174
UCCSD	1.160	2188
ROCCSD	1.161	2164
UMP2	1.121	2923
ROMP2	1.185	1847
	Experimental Results	
	1.171[a]	2069[a]

[a]Values taken from Huber and Herzberg.[110]

dx.doi.org/10.1021/ct400316m | J. Chem. Theory Comput. 2013, 9, 4313−4331

The EOMIP-CCSD(2) method overestimates the bond length by 0.076 Å and underestimates the frequency by 264 cm^{-1}. The EOMIP-CCSD method improves the results, but still shows large error ($|\Delta r_e|$ = 0.069 Å and ($|\Delta \omega_e|$ = 192 cm^{-1}), compared to the experiment. This trend gets reversed in larger basis sets: the EOMIP-CCSD(2) method gives the best agreement with the experiment for both bond length ($|\Delta r_e|$ = 0.007 Å) and vibrational frequency ($|\Delta \omega_e|$ = 64 cm^{-1}) in the aug-cc-pVQZ basis set. The EOMIP-CCSD method slightly underestimates the bond length ($|\Delta r_e|$ = 0.010 Å) and overestimates the frequency ($|\Delta \omega_e|$ = 105 cm^{-1}). The performance of the single-reference coupled-cluster methods is similar to that of the EOMIP-CCSD method, with regard to both bond length and IR frequency. The spin contamination of the UMP2 wave function introduces very large errors in bond length ($|\Delta r_e|$ = 0.050 Å) and IR frequency ($|\Delta \omega_e|$ = 854 cm^{-1}) . The ROMP2 method shows significant improvement over the UMP2 method, but the bond length ($|\Delta r_e|$ = 0.014 Å) and IR frequency ($|\Delta \omega_e|$ = 222 cm^{-1}) still deviate significantly from the experiment.[110]

The F_2^+ shows a T1 diagnosis value of 0.013, which makes it a suitable candidate for single-reference treatment. Table 10 shows that, in the aug-cc-pVDZ basis set, the EOMIP-CCSD(2) method reproduces the experimental[110] bond length and frequency with absolute accuracy. The EOMIP-CCSD method also gives comparable performance for bond length and IR frequency. However, the single-reference coupled-cluster methods underestimate the bond length and overestimate the IR frequency. The UMP2 and ROMP2 methods also overestimate the bond length by a large value (0.073 and 0.115 Å, respectively), but give IR frequencies with accuracy comparable to that of their coupled-cluster analogues. The UMP2 method overestimates the experimental frequency by 51 cm^{-1}, whereas the ROMP2 method underestimates the frequency by 68 cm^{-1}. In the aug-cc-pVTZ and aug-cc-pVQZ basis sets, both the EOM and single-reference coupled-cluster methods underestimate the bond length and overestimate the frequency. The UCCSD and ROCCSD methods, in the aug-cc-pVQZ basis set, give significant error in bond length ($|\Delta r_e|$ = 0.041 and 0.040 Å, respectively), as well as in frequency ($|\Delta \omega_e|$ = 166 and 170 cm^{-1}, respectively). The EOMIP-CCSD(2) method gives better performance than the single-reference coupled-cluster method, although it continues to underestimate the bond length ($|\Delta r_e|$ = 0.027 Å), and overestimates the harmonic vibrational frequency ($|\Delta \omega_e|$ = 105 cm^{-1}). The EOM-CCSD method gives a performance similar to that of the EOMIP-CCSD(2) method, in both the aug-cc-pVTZ and aug-cc-pVQZ basis sets. The UHF- and ROHF-based MBPT(2) methods overestimate the bond length and underestimate the IR frequency. The UMP2 shows a surprisingly accurate bond length of 1.341 Å and leads to an IR frequency that has accuracy comparable to that of the single-reference coupled-cluster method. However, the ROMP2 method performs very poorly for both bond length ($|\Delta r_e|$ = 0.047 Å) and IR frequency ($|\Delta \omega_e|$ = 285 cm^{-1}) .

Table 10. Geometry and Harmonic Vibrational Frequency of F_2^+

method	bond length (Å)	frequency, ω (cm^{-1})
aug-cc-pVDZ Basis Set		
EOMIP-CCSD(2)	1.322	1081
EOMIP-CCSD	1.326	1065
UCCSD	1.312	1128
ROCCSD	1.310	1133
UMP2	1.395	1124
ROMP2	1.437	1005
aug-cc-pVTZ		
EOMIP-CCSD(2)	1.299	1174
EOMIP-CCSD	1.299	1168
UCCSD	1.286	1230
ROCCSD	1.285	1234
UMP2	1.347	890
ROMP2	1.374	781
aug-cc-pVQZ		
EOMIP-CCSD(2)	1.295	1178
EOMIP-CCSD	1.295	1176
UCCSD	1.281	1239
ROCCSD	1.280	1243
UMP2	1.343	897
ROMP2	1.369	788
Experimental Results		
	1.322[a]	1073[a]

[a]Values taken from Huber and Herzberg.[110]

CO^+ is isoelectronic with N_2^+, but shows significant multi-reference character (T1 value = 0.046). Table 11 shows that, in the aug-cc-pVDZ basis set, the EOM and the single-reference coupled-cluster methods overestimate the bond length. For IR frequency, the EOMIP-CCSD(2) method gives the best agreement with the experiment[110] ($|\Delta \omega_e|$ = 7 cm^{-1}), whereas the EOMIP-CCSD and single-reference coupled-cluster methods result in overestimation of the frequency. The UMP2 method underestimates the bond length ($|\Delta r_e|$ = 0.016 Å) and overestimates the frequency ($|\Delta \omega_e|$ = 636 cm^{-1}) by a considerable margin. The ROMP2 method shows greater error

Table 11. Geometry and Harmonic Vibrational Frequency of CO^+

method	bond length (Å)	frequency, ω (cm^{-1})
aug-cc-pVDZ Basis Set		
EOMIP-CCSD(2)	1.123	2221
EOMIP-CCSD	1.122	2257
UCCSD	1.124	2248
ROCCSD	1.123	2259
UMP2	1.100	2850
ROMP2	1.139	2065
aug-cc-pVTZ Basis Set		
EOMIP-CCSD(2)	1.109	2282
EOMIP-CCSD	1.106	2324
UCCSD	1.108	2322
ROCCSD	1.108	2327
UMP2	1.089	2881
ROMP2	1.124	2129
aug-cc-pVQZ Basis Set		
EOMIP-CCSD(2)	1.108	2288
EOMIP-CCSD	1.104	2331
UCCSD	1.106	2330
ROCCSD	1.106	2333
UMP2	1.088	2888
ROMP2	1.122	2132
Experimental Results		
	1.115[a]	2214[a]

[a]Values taken from Huber and Herzberg.[110]

dx.doi.org/10.1021/ct400316m | J. Chem. Theory Comput. 2013, 9, 4313−4331

than the UMP2 method, with regard to bond length ($|\Delta r_e|$ = 0.023 Å), but gives a better result for harmonic vibrational frequency ($|\Delta\omega_e|$ = 149 cm^{-1}). In the aug-cc-pVTZ basis set, the bond length decreases and the IR frequency increases for all of the methods. The EOMIP-CCSD(2) method gives the best agreement with experiment for bond length ($|\Delta r_e|$ = 0.006 Å), as well as IR frequency ($|\Delta\omega_e|$ = 66 cm^{-1}). The EOMIP-CCSD method, as well as the single-reference coupled-cluster method, show inferior performance than the EOMIP-CCSD(2) method in the aug-cc-pVTZ basis set. The UMP2 method severely underestimates the bond length ($|\Delta r_e|$ = 0.027 Å) and overestimates the frequency ($|\Delta\omega_e|$ = 666 cm^{-1}). However, the ROMP2 method gives surprisingly good performance for the bond length ($|\Delta r_e|$ = 0.009 Å) as well as the vibrational frequency ($|\Delta\omega_e|$ = 79 cm^{-1}). The same trend holds in the aug-cc-pVQZ basis set, and the bond length and IR frequency show very small deviations from that determined in the aug-cc-pVTZ basis set.

Table 12. Comparison of the Maximum, Minimum, and Average Absolute Deviation Values of the Computed (aug-cc-pVQZ Basis Set) Equilibrium Bond Lengths from the Experiment

	Bond Length, $\|\Delta r_e\|$ (Å)		
method	min	max	average absolute deviation, AAD
IP-EOM-CCSD(2)	0.004	0.027	0.010
EOM-IP-CCSD	0.000	0.027	0.013
UCCSD	0.006	0.088	0.030
ROCCSD	0.006	0.058	0.016
UMP2	0.012	0.075	0.038
ROMP2	0.004	0.047	0.019

Table 13. Comparison of the Maximum, Minimum, and Average Absolute Deviation Values of the Computed (aug-cc-pVQZ Basis Set) Harmonic Vibrational Frequencies from the Experiment

	Harmonic Vibrational Frequencies, $\|\Delta\omega_e\|$ (cm^{-1})		
method	min	max	average absolute deviation, AAD
IP-EOM-CCSD(2)	23	317	111
EOM-IP-CCSD	52	300	124
UCCSD	17	722	233
ROCCSD	40	487	155
UMP2	25	1337	482
ROMP2	6	634	197

E. Error Analysis. Tables 12 and 13 present the minimum, maximum, and average absolute deviations of the computed (in the aug-cc-pVQZ basis set) bond lengths and harmonic vibrational frequencies from the experiment, for all of the molecules investigated in the paper. Among all the methods used in this work, the EOMIP-CCSD(2) method shows the lowest average absolute deviation for bond length ($|\Delta r_e|$ = 0.010 Å) as well as harmonic vibrational frequency ($|\Delta\omega_e|$ = 111 cm^{-1}); whereas the UCCSD and UMP2 methods show the highest maximum absolute deviations for bond length and harmonic vibrational frequency, respectively. Figure 2 and 3 reveal that the EOMIP-CCSD(2) method gives the best performance for both bond length and IR frequency; these values are very close to (and even better than, in some cases) the EOMIP-CCSD method, despite the latter being computationally more demanding. It is followed, in order of decreasing accuracy, by the ROCCSD method, the ROMP2 method, the UCCSD method, and, lastly, the UMP2 method.

F. Some More Test Cases. After gaining some confidence about the reliability of the EOMIP-CCSD(2) method for structure and IR frequency, we proceed to investigate some larger doublet radicals and dimer radical cations. The latter often show serious symmetry breaking and spin-contamination problems, as previously reported by Krylov and coworkers[111,112] as test cases for estimating the accuracy of the EOMIP-based methods. We compare the structural parameters and IR frequencies calculated using the EOMIP-CCSD(2) method with those obtained using the standard EOMIP-CCSD method, in different basis sets.

Water Dimer Cation. Ionization introduces considerable change in the electronic structure of water dimer cation and leads to the formation of the $OH\cdots H_3O^+$ complex, as seen from Figure 4. The structural parameters are reproduced quite well by the EOMIP-CCSD(2) method. The AAD values in both the bond length and bond angle are 0.013 Å and 0.20°, respectively.

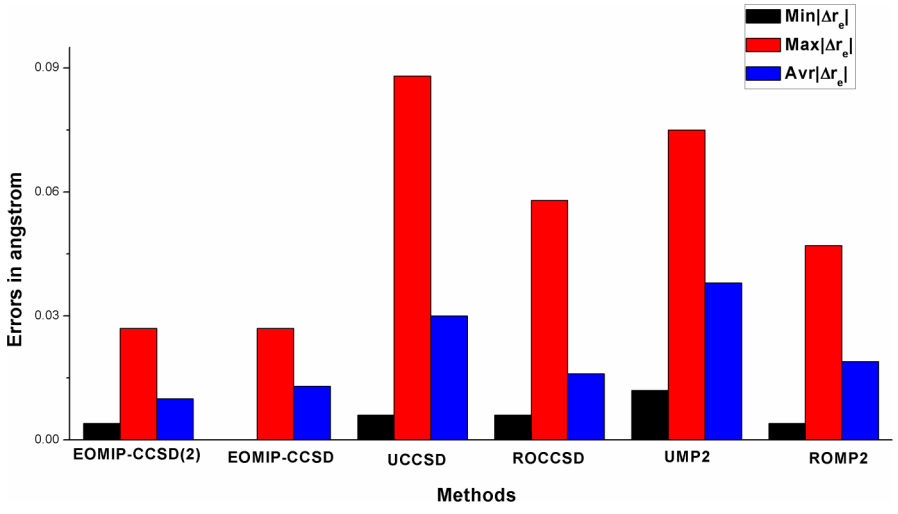

Figure 2. Comparison of the maximum, minimum, and average absolute deviations of the computed (aug-cc-pVQZ basis set) bond length from the experiment.

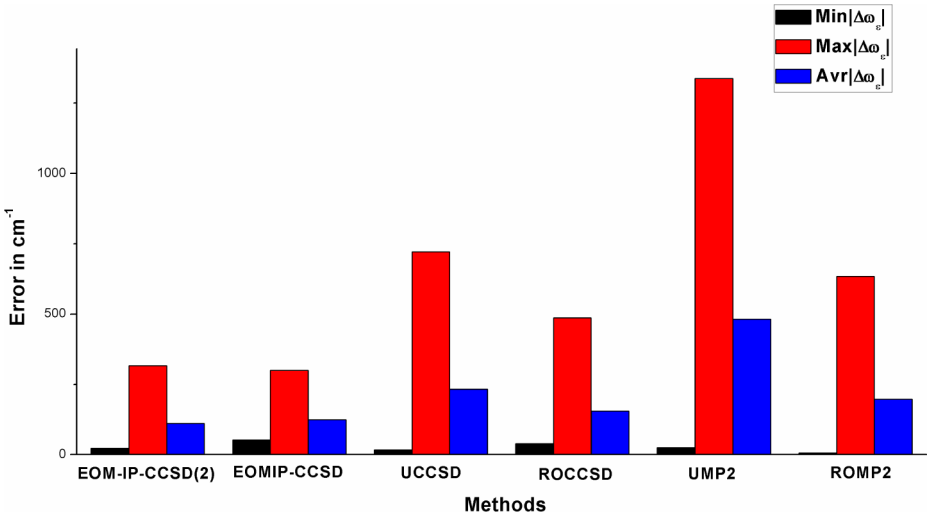

Figure 3. Comparison of the maximum, minimum, and average absolute deviation of the computed (aug-cc-pVQZ basis set) harmonic vibrational frequency from the experiment.

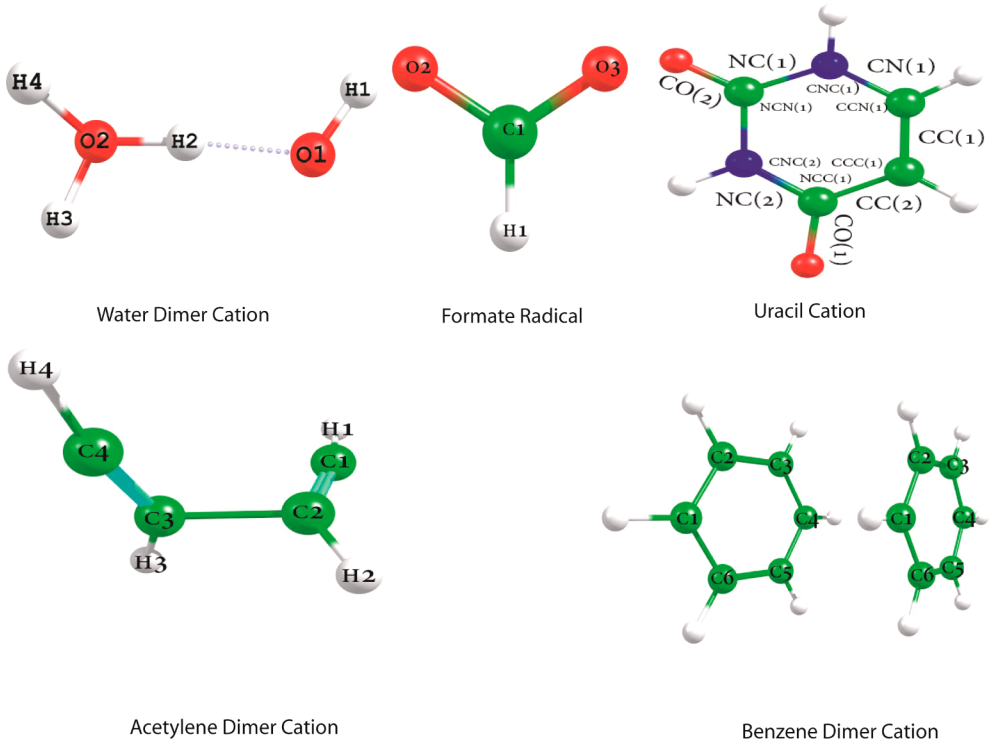

Figure 4. Larger radicals and dimer cations.

Bond lengths shrink, upon moving from the aug-cc-pVDZ basis set to the aug-cc-pVTZ basis set, in both the EOMIP-CCSD(2) and EOMIP-CCSD methods. However, the change from the aug-cc-pVTZ basis set to the aug-cc-pVQZ basis set is very small. An important thing to notice is that the errors observed in the EOMIP-CCSD(2) method, relative to those observed in the EOMIP-CCSD method are not sensitive to the basis set, as one might expect due to the different level of electron correlation included in the reference state of both methods.

The IR frequencies obtained in EOMIP-CCSD(2) method also show negligible deviation from those obtained using the EOMIP-CCSD method, and the average absolute error is quite insensitive to the basis set used. The geometrical parameters and harmonic vibrational frequencies of the water dimer cation are given in Tables 14 and 15, respectively.

Formate Radical. The formate radical has a C_{2v} symmetry, and its electronic wave function belongs to the B_2 irreducible representation. The displacement of the nuclei along the asymmetric stretching mode leads to the coupling of the ground state with a low-lying $^2A_1$ state (second-order Jahn–Teller interaction), which complicates its electronic structure. Therefore, an accurate description of the wave function requires a balanced treatment between the two degenerate states, so the system acts as a sensitive test case for ab initio methods.

dx.doi.org/10.1021/ct400316m | J. Chem. Theory Comput. 2013, 9, 4313–4331

Table 14. Geometrical Parameters of the Water Dimer Cation

	aug-cc-pVDZ			aug-cc-pVTZ			aug-cc-pVQZ
	EOMIP-CCSD	EOMIP-CCSD(2)	error	EOMIP-CCSD	EOMIP-CCSD(2)	error	EOMIP-CCSD(2)
bond length (Å)							
H1−O1	0.983	0.982	0.001	0.975	0.974	0.001	0.973
H2−O1	1.446	1.482	0.036	1.425	1.459	−0.034	1.458
O1−O2	2.495	2.523	0.028	2.470	2.497	−0.027	2.495
H3−O2	0.974	0.977	0.003	0.968	0.971	−0.003	0.970
H4−O2	0.974	0.977	0.003	0.967	0.971	−0.004	0.970
AAD[a]	0.013			0.013			
bond angle (deg)							
H1−O1−H2	121.18	121.39	0.11	121.8	122.08	−0.25	122.65
H3−O2−H4	109.67	109.59	0.08	110.3	110.13	0.14	110.29
AAD[b]	0.20			0.20			

[a]Average absolute deviation of bond length, $|\Delta r_e|$. [b]Average absolute deviation of bond angle, $|\Delta_{angle}|$.

Table 15. Harmonic Vibrational Frequencies of the Water Dimer Cation

	Harmonic Vibrational Frequencies (cm^{-1})						
	aug-cc-pVDZ			aug-cc-pVTZ			aug-cc-pVQZ
	EOMIP-CCSD	EOMIP-CCSD(2)	error	EOMIP-CCSD	EOMIP-CCSD(2)	error	EOMIP-CCSD(2)
1	105	99	6	107	102	5	107
2	383	369	14	381	370	11	376
3	410	387	23	425	400	25	396
4	513	492	21	529	510	19	503
5	632	605	27	634	605	29	601
6	1068	1006	62	1072	1013	59	1005
7	1641	1624	17	1669	1650	19	1647
8	1733	1693	40	1766	1723	43	1712
9	2320	2494	174	2325	2490	165	2493
10	3649	3650	1	3707	3696	11	3698
11	3701	3699	2	3756	3749	7	3754
AAD[a]	35			36			

[a]Average absolute deviation of harmonic vibrational frequency, $|\Delta\omega_e|$.

Table 16. Geometrical Parameters of the Formate Radical

	aug-cc-pVDZ			aug-cc-pVTZ			aug-cc-pVQZ
	EOMIP-CCSD	EOMIP-CCSD(2)	error	EOMIP-CCSD	EOMIP-CCSD(2)	error	EOMIP-CCSD(2)
bond length (Å)							
C1−O2	1.261	1.266	0.005	1.246	1.252	0.006	1.250
C1−O3	1.261	1.266	0.005	1.246	1.252	0.006	1.250
H1−C	1.102	1.099	0.003	1.085	1.084	0.001	1.086
AAD[a]	0.004			0.004			
bond angle (deg)							
O−C1−O	112.40	110.80	1.6	112.45	110.90	1.55	110.92
H1−C1−O	123.80	124.59	0.79	123.77	124.55	0.78	124.54
AAD[b]	1.19			1.16			

[a]Average absolute deviation of bond length, $|\Delta r_e|$. [b]Average absolute deviation of bond angle, $|\Delta_{angle}|$.

Table 16 shows that the EOMIP-CCSD(2) method reproduces the bond lengths and bond angles, obtained using the EOMIP-CCSD method, with reasonable accuracy in both the aug-cc-pVDZ and aug-cc-pVTZ basis sets. For both methods, all the bond lengths shrink upon moving from the aug-cc-pVDZ basis set to the aug-cc-pVTZ basis set. In the aug-cc-pVQZ basis set, we have performed the calculations only using the EOMIP-CCSD(2) method, and the values show very little deviation from that in the aug-cc-pVTZ basis set. The average absolute deviation in bond lengths and bond angles are 0.004 Å and 1.19°, respectively, and these values are insensitive to the basis set used.

dx.doi.org/10.1021/ct400316m | J. Chem. Theory Comput. 2013, 9, 4313−4331

Table 17. Harmonic Vibrational Frequencies of the Formate Radical

	Harmonic Vibrational Frequencies (cm^{-1})						
	aug-cc-pVDZ			aug-cc-pVTZ			aug-cc-pVQZ
	EOMIP-CCSD	EOMIP-CCSD(2)	error	EOMIP-CCSD	EOMIP-CCSD(2)	error	EOMIP-CCSD(2)
1	652	634	18	665	643	22	648
2	1021	1001	20	1052	1028	24	1024
3	1073	1037	36	1107	1052	55	1052
4	1296	1274	22	1308	1280	28	1293
5	1489	1467	22	1529	1498	31	1502
6	3152	3176	24	3164	3186	22	3188
AAD[a]|	24			30			

[a]Average absolute deviation of harmonic vibrational frequency, $|\Delta\omega_e|$.

Table 18. Geometrical Parameters of the Uracil Cation

	cc-pVDZ			cc-pVTZ
	EOMIP-CCSD	EOMIP-CCSD(2)	|error|	EOMIP-CCSD(2)
bond length (Å)				
C−C(1)	1.372	1.384	0.012	1.367
C−N(1)	1.358	1.348	0.010	1.335
N−C(1)	1.390	1.397	0.007	1.384
C−N(2)	1.431	1.429	0.002	1.415
N−C(2)	1.344	1.341	0.003	1.328
C−C(2)	1.432	1.412	0.020	1.394
C−O(1)	1.277	1.305	0.028	1.298
C−O(2)	1.192	1.195	0.003	1.188
AAD[a]	0.011			
bond angle (deg)				
C−C−N(1)	122.75	122.36	0.390	122.42
C−N−C(1)	124.33	124.80	0.470	124.62
N−C−N(1)	112.23	111.55	0.680	111.73
C−N−C(2)	124.73	124.77	0.040	124.36
N−C−C(1)	120.38	121.13	0.750	121.49
C−C−C(1)	115.57	115.37	0.20	115.36
AAD[b]	0.42			

[a]Average absolute deviation of bond length, $|\Delta r_e|$. [b]Average absolute deviation of bond angle, $|\Delta_{angle}|$.

Table 19. Harmonic Vibrational Frequencies of the Uracil Cation

	Harmonic Vibrational Frequencies (cm^{-1})			
	cc-pVDZ			cc-pVTZ
	EOMIP-CCSD	EOMIP-CCSD(2)	|error|	EOMIP-CCSD(2)
1	118	129	11	139
2	156	167	11	181
3	346	341	5	245
4	367	368	1	390
5	504	500	4	487
6	523	520	3	522
7	560	554	6	544
8	654	655	1	662
9	689	705	16	668
10	703	722	19	716
11	773	767	6	735
12	786	779	7	792
13	839	831	8	794
14	963	954	9	863
15	1011	1004	7	973
16	1015	1025	10	1045
17	1126	1115	11	1051
18	1220	1195	25	1115
19	1245	1246	1	1245
20	1365	1337	28	1281
21	1401	1376	25	1352
22	1460	1466	6	1461
23	1522	1524	2	1502
24	1577	1582	5	1623
25	1680	1656	24	1650
26	1936	1932	4	1917
27	3266	3275	9	3269
28	3307	3320	13	3335
29	3573	3547	26	3552
30	3618	3592	26	3599
AAD[a]	11			

[a]Average absolute deviation of harmonic vibrational frequency, $|\Delta\omega_e|$.

The IR frequencies also show very good agreement with those obtained using the EOMIP-CCSD method, with average absolute deviations of 23 cm^{-1} and 30 cm^{-1}, in the aug-cc-pVDZ and aug-cc-pVTZ basis sets, respectively. The harmonic vibrational frequencies of the formate radical are given in Table 17.

Uracil Cation. The investigation of ionization-induced structural change of DNA and RNA bases constitutes an important branch of radiation biology. We have investigated the geometry and vibrational frequencies of the uracil cation, which is the ionized form of the smallest of the RNA bases, so that comparison with EOMIP-CCSD method can be made in a reasonable basis set.

The uracil cation has eight different bonds between the heavy atoms, as depicted in Figure 4. The bond length and bond angle in the EOMIP-CCSD(2) method, versus the EOMIP-CCSD method in the cc-pVDZ basis set, is summarized in Table 18. The EOMIP-CCSD(2) method shows reasonable agreement with the EOMIP-CCSD method, as indicated by the small average absolute deviations in bond length (0.011 Å) and bond angle (1.13°). In the EOMIP-CCSD(2) method, the bond lengths shrink, upon moving from the cc-pVDZ basis set to the cc-pVTZ basis set. Table 19 shows that both methods are in excellent agreement for the IR frequencies, exhibiting a maximum value of 28 cm^{-1} and an average absolute deviation of 11 cm^{-1}.

dx.doi.org/10.1021/ct400316m | J. Chem. Theory Comput. 2013, 9, 4313−4331

Table 20. Geometrical Parameters of the Acetylene Dimer Cation

	cc-pVDZ			cc-pVTZ
	EOMIP-CCSD	EOMIP-CCSD(2)	|error|	EOMIP-CCSD(2)
bond length (Å)				
H1−C1	1.088	1.087	0.001	1.068
C1−C2	1.270	1.271	0.001	1.250
C2−H2	1.093	1.094	0.001	1.074
C2−C3	1.705	1.692	0.013	1.681
C3−H3	1.093	1.094	0.001	1.074
C3−C4	1.270	1.271	0.001	1.250
C4−H4	1.088	1.086	0.002	1.068
AAD[a]	0.003			
bond angle (deg)				
H1−C1−C2	169.14	170.09	0.95	170.58
H2−C2−C1	139.63	135.62	4.01	136.86
C1−C2−C3	107.71	114.24	6.53	113.42
H3−C3−C4	139.63	135.62	4.01	136.86
H4−C4−C3	169.14	170.09	0.95	170.58
AAD[b]	3.39			

[a]Average absolute deviation of bond length, $|\Delta r_e|$. [b]Average absolute deviation of bond angle, $|\Delta_{angle}|$.

Table 21. Harmonic Vibrational Frequencies of Acetylene Dimer Cation

	Harmonic Vibrational Frequencies (cm^{-1})			
	cc-pVDZ			cc-pVTZ
	EOMIP-CCSD	EOMIP-CCSD(2)	|ERROR|	EOMIP-CCSD(2)
1	99	136	37	139
2	174	217	43	211
3	222	270	48	247
4	469	551	82	537
5	567	641	74	673
6	605	652	47	683
7	710	655	55	690
8	716	711	5	732
9	775	754	21	766
10	785	756	29	769
11	1005	985	20	998
12	1070	1058	12	1076
13	1760	1800	40	1812
14	1794	1817	23	1830
15	3275	3266	9	3271
16	3275	3267	8	3272
17	3373	3385	12	3394
18	3380	3399	19	3407
AAD[a]	32			

[a]Average absolute deviation of harmonic vibrational frequency, $|\Delta\omega_e|$.

Acetylene Dimer Cation. Acetylene dimer cations are believed to be the building blocks of large polycyclic aromatic hydrocarbon in interstellar clouds. High-energy interstellar conditions make the scope of the experiments very limited, and ab initio methods provide a valuable tool for characterization of these compounds.

Table 20 compares the structural parameters calculated using the EOMIP-CCSD(2) and EOMIP-CCSD methods in the cc-pVDZ basis set. The average absolute deviations in bond length and bond angles are 0.003 Å and 3.39°, respectively. The bond lengths in the EOMIP-CCSD(2) method shrink, upon moving to the cc-pVTZ basis set. Table 21 shows that the average absolute deviation in the frequency is only 32 cm^{-1}, which indicates the power of the EOMIP-CCSD(2) method to reproduce the IR spectra computed using the expensive EOMIP-CCSD method, with reasonable accuracy.

Table 22. Geometrical Parameters of the *y*-Displaced Benzene Dimer Cation

	6-31G			6-31G*
	EOMIP-CCSD	EOMIP-CCSD(2)	|error|	EOMIP-CCSD(2)
bond length (Å)				
C1−C2	1.424	1.424	0	1.407
C2−C3	1.424	1.424	0	1.407
C3−C4	1.401	1.400	0.001	1.385
C4−C5	1.436	1.437	0.001	1.420
C5−C6	1.436	1.437	0.001	1.420
C6−C1	1.401	1.400	0.001	1.385
AAD[a]		0.01		
bond angle (deg)				
C1−C2−C3	120.92	121.04	0.12	121.20
C2−C3−C4	119.72	119.66	0.06	119.56
C3−C4−C5	119.76	119.80	0.04	119.74
C4−C5−C6	119.77	119.89	0.12	120.03
C5−C6−C1	119.76	119.80	0.04	119.74
C6−C1−C2	119.72	119.66	0.06	119.56
AAD[b]		0.07		

[a]Average absolute deviation of bond length, $|\Delta r_e|$. [b]Average absolute deviation of bond angle, $|\Delta_{angle}|$.

Benzene Dimer Cation. The benzene dimer cation has three possible structures: *x*-displaced structure, *y*-displaced structure, and T-shaped structure. We have taken the *y*-displaced structure as our test case. Table 22 shows that ionization-induced structural changes using the EOMIP-CCSD method is reproduced with excellent accuracy in the EOMIP-CCSD(2) method, which is indicated by small average absolute deviations in the bond length (0.001 Å) and bond angles (0.07°) in the 6-31G basis set. The bond lengths shrink, using the EOMIP-CCSD(2) method, upon moving to the 6-31G* basis set. Table 23 shows that the IR frequencies computed using the EOMIP-CCSD(2) method show excellent agreement with those in the EOMIP-CCSD method and the absolute deviation in frequency is only 16 cm^{-1}.

4. CONCLUSIONS

We have presented a benchmark study on the performance of the EOMIP-CCSD(2) method for geometry and vibrational frequencies of doublet radicals. The method, being naturally spin-adapted and equipped to address multireference situations, can avoid the problems associated with the standard single-reference ab initio treatment of open-shell radicals. In addition to

Table 23. Harmonic Vibrational Frequencies of the *y*-Displaced Benzene Dimer Cation

	Harmonic Vibrational Frequencies (cm^{-1})			
	cc-pVDZ			cc-pVTZ
	EOMIP-CCSD	EOMIP-CCSD(2)	|ERROR|	EOMIP-CCSD(2)
1	29	32	2	34
2	46	47	0	51
3	66	73	8	69
4	76	79	3	82
5	93	101	8	109
6	178	185	7	200
7	370	366	4	367
8	372	367	5	368
9	373	371	2	375
10	384	383	1	390
11	546	521	24	522
12	554	536	18	540
13	599	601	2	586
14	601	602	1	589
15	607	608	1	598
16	623	624	1	614
17	703	704	1	716
18	712	714	3	726
19	822	818	4	835
20	827	823	3	839
21	856	859	4	882
22	866	862	4	892
23	905	898	7	923
24	912	899	13	930
25	928	904	24	937
26	930	906	24	939
27	938	928	10	956
28	941	929	12	958
29	969	968	1	995
30	988	985	4	1013
31	1030	1032	1	1022
32	1032	1034	2	1025
33	1038	1046	7	1053
34	1039	1046	7	1055
35	1063	1067	4	1086
36	1065	1069	4	1087
37	1192	1205	13	1207
38	1204	1214	10	1214
39	1226	1237	12	1221
40	1227	1237	10	1225
41	1228	1240	12	1230
42	1237	1247	10	1236
43	1337	1417	80	1396
44	1350	1420	70	1397
45	1412	1420	8	1492
46	1412	1442	29	1513
47	1503	1502	2	1514
48	1504	1505	1	1522
49	1504	1506	2	1523
50	1515	1512	4	1541
51	1554	1553	0	1592
52	1558	1555	3	1593
53	1589	1584	5	1625
54	1644	1634	11	1680
55	3159	3200	41	3248
56	3160	3201	41	3249
57	3169	3214	45	3260
58	3169	3214	45	3261
59	3170	3214	44	3262
60	3173	3217	44	3263
61	3180	3223	43	3267
62	3182	3226	44	3270
63	3188	3232	43	3274
64	3189	3232	43	3275
65	3195	3238	43	3278
66	3196	3240	43	3278
AAD[a]		16		

[a]Average absolute deviation of harmonic vibrational frequency, $|\Delta\omega_e|$.

that, the method is computationally less expensive than the standard EOMIP-CCSD and single-reference coupled-cluster methods, in terms of both computational scaling as well as storage requirements. The performance of the method is benchmarked, in a hierarchy of Dunning's correlation-consistent aug-cc-pVXZ (X = D, T, Q) basis sets, on a variety of doublet radicals, which are previously reported to be challenging cases for standard ab initio methods. We have compared our results with the EOMIP-CCSD method, the UHF- and ROHF-based coupled-cluster methods, and MBPT(2) method. The computed results demonstrate that the EOMIP-CCSD(2) method provides reasonable agreement with the experimental geometry and IR frequency. The calculated bond lengths and frequencies are strongly dependent on the basis sets used. The bond lengths decrease and IR frequencies shift to higher values upon changing the basis set from the aug-cc-pVDZ basis set to the aug-cc-pVTZ basis set. The change in the results is negligible upon moving from the aug-cc-pVTZ basis set to the aug-cc-pVQZ basis set; hence, the results in the aug-cc-pVQZ basis set can be taken as the complete basis set limit results. We have calculated the minimum, maximum, and average absolute deviations from the experiment for all of the methods, in the aug-cc-pVQZ basis set. The EOMIP-CCSD(2) method shows the smallest average absolute deviation in bond length ($|\Delta r_e| = 0.010$ Å), as well as in IR frequency ($|\Delta\omega_e| = 111$ cm^{-1}). The method performs similar to that of the standard EOMIP-CCSD method, even better in some particular cases, despite the latter being more computationally expensive. The UHF reference-based MBPT(2) and CCSD methods fail to reproduce even the qualitative trends for most of the cases, which is indicated by the high value of the maximum and average absolute deviations in bond length and IR frequency. However, the ROHF-based CCSD and MBPT(2) method shows comparatively better results than the UHF-based CCSD and MBPT(2) method, but performs poorly compared to the EOMIP-CCSD(2) method. Inclusion of partial triples will obviously improve the results for the single-reference coupled-cluster methods. However, it will also increase the scaling to N^7, which will make the method computationally unfeasible, even for the moderately sized molecules.

Our calculations on the larger radicals and dimer cations show that the geometries and IR frequencies, obtained using the EOMIP-CCSD method, are well-reproduced in the less-expensive EOMIP-CCSD(2) method .

The EOMIP-CCSD(2) method offers an efficient black box approach for the theoretical treatment of doublet radicals and

gives accuracy comparable to the robust EOMIP-CCSD method, at significantly lower computational cost. The method has immense potential to be used in the theoretical treatment of open-shell radicals, biological molecules, and gas-phase clusters. Current EOM-IP-CCSD codes can be used to describe systems as large as a nucleobase tetramer;[66,67] therefore, cutting the scaling can really extend the range of systems. Work is currently underway to study the properties and thermochemistry of DNA base pairs and ionized water clusters.

■ ASSOCIATED CONTENT

Ⓢ Supporting Information

Z-Matrix of the optimized geometries, nuclear repulsion energy, SCF energy, correlation energy, final energy, vibrational frequency, and infrared intensity are given as Supporting Information. This material is available free of charge via the Internet at http://pubs.acs.org.

■ AUTHOR INFORMATION

Corresponding Author

*E-mail: s.pal@ncl.res.in.

Notes

The authors declare no competing financial interest.

■ ACKNOWLEDGMENTS

The authors acknowledge a grant from the CSIR XII[th] Five Year Plan Project on Multiscale Simulations of Material (MSM) and facilities of the Centre of Excellence in Scientific Computing at NCL. A.K.D. thanks the Council of Scientific and Industrial Research (CSIR) for a Senior Research Fellowship. S.P. acknowledges the DST J. C. Bose Fellowship project and a CSIR SSB grant towards completion of the work.

■ REFERENCES

(1) Cizek, J. On the Correlation Problem in Atomic and Molecular Systems. Calculation of Wavefunction Components in Ursell-Type Expansion Using Quantum-Field Theoretical Methods. *J. Chem. Phys.* **1966**, *45*, 4256−4266.

(2) Bartlett, R. J. Many-Body Perturbation Theory and Coupled Cluster Theory for Electron Correlation in Molecules. *Annu. Rev. Phys. Chem.* **1981**, *32*, 359−401.

(3) Adamowicz, L.; Laidig, W. D.; Bartlett, R. J. Analytical gradients for the coupled-cluster method. *Int. J. Quantum Chem.* **1984**, *26*, 245−254.

(4) Salter, E. A.; Trucks, G. W.; Bartlett, R. J. Analytic energy derivatives in many-body methods. I. First derivatives. *J. Chem. Phys.* **1989**, *90*, 1752−1766.

(5) Scheiner, A. C.; Scuseria, G. E.; Rice, J. E.; Lee, T. J.; Schaefer, H. F., III. Analytic evaluation of energy gradients for the single and double excitation coupled cluster (CCSD) wave function: Theory and application. *J. Chem. Phys.* **1987**, *87*, 5361−5373.

(6) Monkhorst, H. J. Calculation of properties with the coupled-cluster method. *Int. J. Quantum Chem.* **1977**, *12*, 421−432.

(7) Besler, B. H.; Scuseria, G. E.; Scheiner, A. C.; Schaefer, H. F., III. A systematic theoretical study of harmonic vibrational frequencies: The single and double excitation coupled cluster (CCSD) method. *J. Chem. Phys.* **1988**, *89*, 360−366.

(8) Koch, H.; Jensen, H. J. A.; Jorgensen, P.; Helgaker, T.; Scuseria, G. E.; Schaefer, H. F., III. Coupled cluster energy derivatives. Analytic Hessian for the closed-shell coupled cluster singles and doubles wave function: Theory and applications. *J. Chem. Phys.* **1990**, *92*, 4924−4940.

(9) Salter, E. A.; Bartlett, R. J. Analytic energy derivatives in many-body methods. II. Second derivatives. *J. Chem. Phys.* **1989**, *90*, 1767−1773.

(10) Knowles, P. J.; Hampel, C.; Werner, H. J. Coupled cluster theory for high spin, open shell reference wave functions. *J. Chem. Phys.* **1993**, *99*, 5219−5227.

(11) Rittby, M.; Bartlett, R. J. An open-shell spin-restricted coupled cluster method: Application to ionization potentials in nitrogen. *J. Phys. Chem.* **1988**, *92*, 3033−3036.

(12) Scuseria, G. E. The open-shell restricted Hartree−Fock singles and doubles coupled-cluster method including triple excitations CCSD(T): Application to C^{+3}. *Chem. Phys. Lett.* **1991**, *176*, 27−35.

(13) Raghavachari, K.; Trucks, G. W.; Pople, J. A.; Head-Gordon, M. A fifth-order perturbation comparison of electron correlation theories. *Chem. Phys. Lett.* **1989**, *157*, 479−483.

(14) Stanton, J. F. Why CCSD(T) works: A different perspective. *Chem. Phys. Lett.* **1997**, *281*, 130−134.

(15) Bartlett, R. J.; Watts, J. D.; Kucharski, S. A.; Noga, J. Non-iterative fifth-order triple and quadruple excitation energy corrections in correlated methods. *Chem. Phys. Lett.* **1990**, *165*, 513−522.

(16) Möller, C.; Plesset, M. S. Note on an Approximation Treatment for Many-Electron Systems. *Phys. Rev.* **1934**, *46*, 618−622.

(17) Lauderdale, W. J.; Stanton, J. F.; Gauss, J.; Watts, J. D.; Bartlett, R. J. Many-body perturbation theory with a restricted open-shell Hartree−Fock reference. *Chem. Phys. Lett.* **1991**, *187*, 21−28.

(18) Lauderdale, W. J.; Stanton, J. F.; Gauss, J.; Watts, J. D.; Bartlett, R. J. Restricted open-shell Hartree−Fock-based many-body perturbation theory: Theory and application of energy and gradient calculations. *J. Chem. Phys.* **1992**, *97*, 6606−6620.

(19) Detailed duscussion on the origin of the problems associated with theroretical treatment of doublet radicals is outside the scope of the present work. References 20 and 21 should be consulted for a elaborate review on the above-mentioned subject.

(20) Stanton, J. F.; Gauss, J. A Discussion of Some Problems Associated with the Quantum Mechanical Treatment of Open-Shell Molecules. In *Advances in Chemical Physics*, Vol. *125*; John Wiley & Sons, Inc.: New York, 2003; pp 101−146.

(21) Szalay, P. G.; Vazquez, J.; Simmons, C.; Stanton, J. F. Triplet instability in doublet systems. *J. Chem. Phys.* **2004**, *121*, 7624−7631.

(22) Andrews, J. S.; Jayatilaka, D.; Bone, R. G. A.; Handy, N. C.; Amos, R. D. Spin contamination in single-determinant wavefunctions. *Chem. Phys. Lett.* **1991**, *183*, 423−431.

(23) Hehre, W. J.; Radom, L.; Schleyer, P. v. R.; Pople, J. A. *Ab Initio Molecular Orbital Theory*: John Wiley & Sons, Inc.: New York, 1986.

(24) Davidson, E. R.; Borden, W. T. Symmetry breaking in polyatomic molecules: Real and artifactual. *J. Phys. Chem.* **1983**, *87*, 4783−4790.

(25) Cizek, J.; Paldus, J. Stability Conditions for the Solutions of the Hartree−Fock Equations for Atomic and Molecular Systems. Application to the Pi-Electron Model of Cyclic Polyenes. *J. Chem. Phys.* **1967**, *47*, 3976−3985.

(26) Thouless, D. J. *The Quantum Mechanics Of Many-Body Systems*; Academic Press: New York, 1961; p 126.

(27) Pearson, R. G. *Symmetry Rules for Chemical Reactions*; Wiley: New York, 1976.

(28) Eisfeld, W. Ab initio calculation of electronic absorption spectra and ionization potentials of C_3H_3 radicals. *Phys. Chem. Chem. Phys.* **2005**, *7*, 3924−3932.

(29) Goddard, J. D.; Handy, N. C.; Schaefer, H. F., III. Gradient techniques for open-shell restricted Hartree–Fock and multiconfiguration self-consistent-field methods. *J. Chem. Phys.* **1979**, *71*, 1525−1530.

(30) Golubeva, A. A.; Pieniazek, P. A.; Krylov, A. I. A new electronic structure method for doublet states: Configuration interaction in the space of ionized 1h and 2h1p determinants. *J. Chem. Phys.* **2009**, *130*, 124113−10.

(31) Gonzalez, M.; Valero, R.; Sayos, R. Ab initio ground potential energy surface ($^3A''$) for the $O(^3P) + N_2O$ reaction and kinetics study. *J. Chem. Phys.* **2001**, *115*, 2540−2549.

(32) Hammond, J. R.; Mazziotti, D. A. Variational reduced-density-matrix calculations on radicals: An alternative approach to open-shell ab initio quantum chemistry. *Phys. Rev. A* **2006**, *73*, 012509.

(33) McLean, A. D.; Lengsfield, B. H., III; Pacansky, J.; Ellinger, Y. Symmetry breaking in molecular calculations and the reliable prediction

of equilibrium geometries. The formyloxyl radical as an example. *J. Chem. Phys.* **1985**, *83*, 3567−3576.
(34) Stanton, J. F.; Gauss, J. A simple correction to final state energies of doublet radicals described by equation-of-motion coupled cluster theory in the singles and doubles approximation. *Theor. Chim. Acta* **1996**, *93*, 303−313.
(35) Andersson, K.; Malmqvist, P. A.; Roos, B. O. Second-order perturbation theory with a complete active space self-consistent field reference function. *J. Chem. Phys.* **1992**, *96*, 1218−1226.
(36) Hirao, K. Multireference Möller-Plesset method. *Chem. Phys. Lett.* **1992**, *190*, 374−380.
(37) Hirao, K. State-specific multireference Möller−Plesset perturbation treatment for singlet and triplet excited states, ionized states and electron attached states of H_2O. *Chem. Phys. Lett.* **1993**, *201*, 59−66.
(38) Malmqvist, P. A.; Rendell, A.; Roos, B. O. The restricted active space self-consistent-field method, implemented with a split graph unitary group approach. *J. Phys. Chem.* **1990**, *94*, 5477−5482.
(39) Lischka, H.; Shepard, R.; Brown, F. B.; Shavitt, I. New implementation of the graphical unitary group approach for multi-reference direct configuration interaction calculations. *Int. J. Quantum Chem.* **1981**, *20*, 91−100.
(40) Meyer, W. *Methods of Electronic Structure Theory.*: Plenum Press: New York, 1977; Vol. *4*, pp 413.
(41) Balkova, A.; Kucharski, S. A.; Meissner, L.; Bartlett, R. J. The multireference coupled-cluster method in Hilbert space: An incomplete model space application to the LiH molecule. *J. Chem. Phys.* **1991**, *95*, 4311−4316.
(42) Chattopadhyay, S.; Sinha Mahapatra, U.; Datta, B.; Mukherjee, D. State-specific multi-reference coupled electron-pair approximation like methods: Formulation and molecular applications. *Chem. Phys. Lett.* **2002**, *357*, 426−433.
(43) Evangelista, F. A.; Allen, W. D.; Schaefer, H. F., III. Coupling term derivation and general implementation of state-specific multireference coupled cluster theories. *J. Chem. Phys.* **2007**, *127*, 024102-17−.
(44) Evangelista, F. A.; Simmonett, A. C.; Allen, W. D.; Schaefer, H. F., III; Gauss, J. Triple excitations in state-specific multireference coupled cluster theory: Application of Mk-MRCCSDT and Mk-MRCCSDT-n methods to model systems. *J. Chem. Phys.* **2008**, *128*, 124104-13−.
(45) Hanrath, M. An exponential multireference wave-function Ansatz. *J. Chem. Phys.* **2005**, *123*, 084102-12.
(46) Jeziorski, B.; Monkhorst, H. J. Coupled-cluster method for multideterminantal reference states. *Phys. Rev. A* **1981**, *24*, 1668−1681.
(47) Kaldor, U.; Haque, A. Open-shell coupled-cluster method: Direct calculation of excitation energies. *Chem. Phys. Lett.* **1986**, *128*, 45−48.
(48) Mukherjee, D.; Pal, S. Use of Cluster Expansion Methods in the Open-Shell Correlation Problem. In *Advances in Quantum Chemistry*; Per-Olov, L. w., Ed.; Academic Press: New York, 1989; Vol. *20*, pp 291−373.
(49) Pal, S.; Rittby, M.; Bartlett, R. J.; Sinha, D.; Mukherjee, D. Molecular applications of multireference coupled-cluster methods using an incomplete model space: Direct calculation of excitation energies. *J. Chem. Phys.* **1988**, *88*, 4357−4366.
(50) Pittner, J.; Nachtigall, P.; Carsky, P.; Masik, J.; Hubac, I. Assessment of the single-root multireference Brillouin–Wigner coupled-cluster method: Test calculations on CH_2, SiH_2, and twisted ethylene. *J. Chem. Phys.* **1999**, *110*, 10275−10282.
(51) Vaval, N.; Pal, S.; Mukherjee, D. Fock space multireference coupled cluster theory: noniterative inclusion of triples for excitation energies. *Theor. Chem. Acc.* **1998**, *99*, 100−105.
(52) Sekino, H.; Bartlett, R. J. A linear response, coupled-cluster theory for excitation energy. *Int. J. Quantum Chem.* **1984**, *26*, 255−265.
(53) Nooijen, M.; Bartlett, R. J. Equation of motion coupled cluster method for electron attachment. *J. Chem. Phys.* **1995**, *102*, 3629−3647.
(54) Stanton, J. F.; Bartlett, R. J. The equation of motion coupled-cluster method. A systematic biorthogonal approach to molecular excitation energies, transition probabilities, and excited state properties. *J. Chem. Phys.* **1993**, *98*, 7029−7039.
(55) Krylov, A. I. Equation-of-Motion Coupled-Cluster Methods for Open-Shell and Electronically Excited Species: The Hitchhiker's Guide to Fock Space. *Annu. Rev. Phys. Chem.* **2008**, *59*, 433−462.
(56) Kowalski, K.; Piecuch, P. The active-space equation-of-motion coupled-cluster methods for excited electronic states: Full EOMCCSDt. *J. Chem. Phys.* **2001**, *115*, 643−651.
(57) Kucharski, S. A.; Wloch, M.; Musial, M.; Bartlett, R. J. Coupled-cluster theory for excited electronic states: The full equation-of-motion coupled-cluster single, double, and triple excitation method. *J. Chem. Phys.* **2001**, *115*, 8263−8266.
(58) Prashant, U. M.; John, F. S.; Anna, I. K. Perturbative triples correction for the equation-of-motion coupled-cluster wave functions with single and double substitutions for ionized states: Theory, implementation, and examples. *J. Chem. Phys.* **2009**, *131*, 114112.
(59) Stanton, J. F.; Gauss, J. Analytic energy derivatives for ionized states described by the equation-of-motion coupled cluster method. *J. Chem. Phys.* **1994**, *101*, 8938−8944.
(60) Levchenko, S. V.; Wang, T.; Krylov, A. I. Analytic gradients for the spin-conserving and spin-flipping equation-of-motion coupled-cluster models with single and double substitutions. *J. Chem. Phys.* **2005**, *122*, 224106-11−.
(61) Stanton, J. F. Many-body methods for excited state potential energy surfaces. I. General theory of energy gradients for the equation-of-motion coupled-cluster method. *J. Chem. Phys.* **1993**, *99*, 8840−8847.
(62) Kállay, M.; Gauss, J. Calculation of excited-state properties using general coupled-cluster and configuration−interaction models. *J. Chem. Phys.* **2004**, *121*, 9257−9269.
(63) Saeh, J. C.; Stanton, J. F. Application of an equation-of-motion coupled cluster method including higher-order corrections to potential energy surfaces of radicals. *J. Chem. Phys.* **1999**, *111*, 8275−8285.
(64) Stanton, J. F. On the vibronic level structure in the NO_3 radical. I. The ground electronic state. *J. Chem. Phys.* **2007**, *126*, 134309−20.
(65) Stanton, J. F. On the vibronic level structure in the NO_3 radical: II. Adiabatic calculation of the infrared spectrum. *Mol. Phys.* **2009**, *107*, 1059−1075.
(66) Bravaya, K. B.; Epifanovsky, E.; Krylov, A. I. Four Bases Score a Run: Ab Initio Calculations Quantify a Cooperative Effect of H-Bonding and Ï€-Stacking on the Ionization Energy of Adenine in the AATT Tetramer. *J. Phys. Chem. Lett. 3*, 2726−2732.
(67) Epifanovsky, E.; Wormit, M.; Kuś, T.; Landau, A.; Zuev, D.; Khistyaev, K.; Manohar, P.; Kaliman, I.; Dreuw, A.; Krylov, A. I. New implementation of high-level correlated methods using a general block-tensor library for high-performance electronic structure calculations. *J. Comput. Chem.*, n/a-n/a.
(68) Stanton, J. F.; Gauss, J. Perturbative treatment of the similarity transformed Hamiltonian in equation-of-motion coupled-cluster approximations. *J. Chem. Phys.* **1995**, *103*, 1064−1076.
(69) Watts, J. D.; Bartlett, R. J. The coupled-cluster single, double, and triple excitation model for open-shell single reference functions. *J. Chem. Phys.* **1990**, *93*, 6104−6105.
(70) Noga, J.; Bartlett, R. J. The full CCSDT model for molecular electronic structure. *J. Chem. Phys.* **1987**, *86*, 7041−7050.
(71) Oliphant, N.; Adamowicz, L. Coupled-cluster method truncated at quadruples. *J. Chem. Phys.* **1991**, *95*, 6645−6651.
(72) Kucharski, S. A.; Bartlett, R. J.; Per-Olov, L., Fifth-Order Many-Body Perturbation Theory and Its Relationship to Various Coupled-Cluster Approaches. In *Adv. Quantum Chem.*, Academic Press: 1986; Vol. Vol. *18*, pp 281−344.
(73) Musial, M.; Bartlett, R. J. Multireference Fock-space coupled-cluster and equation-of-motion coupled-cluster theories: The detailed interconnections. *J. Chem. Phys.* **2008**, *129*, 134105−12.
(74) Vaval, N.; Ghose, K. B.; Pal, S.; Mukherjee, D. Fock-space multireference coupled-cluster theory. fourth-order corrections to the ionization potential. *Chem. Phys. Lett.* **1993**, *209*, 292−298.
(75) Musial, M., Multireference Fock space coupled cluster method in the effective and intermediate Hamiltonian formulation for the (2,0) sector. *J. Chem. Phys. 136*, 134111-14.

(76) Musial, M.; Kucharski, S. A.; Zerzucha, P.; Kuś, T.; Bartlett, R. J. Excited and ionized states of the ozone molecule with full triples coupled cluster methods. *J. Chem. Phys.* **2009**, *131*, 194104−10.
(77) Bag, A.; Manohar, P. U.; Vaval, N.; Pal, S. First- and second-order electrical properties computed at the FSMRCCSD level for excited states of closed-shell molecules using the constrained-variational approach. *J. Chem. Phys.* **2009**, *131*, 024102−8.
(78) Barysz, M.; Rittby, M.; Bartlett, R. J. Fock space multi-reference coupled-cluster study of excitation energies and dipole oscillator strengths of ozone. *Chem. Phys. Lett.* **1992**, *193*, 373−379.
(79) Bhattacharya, D.; Vaval, N.; Pal, S., Electronic transition dipole moments and dipole oscillator strengths within Fock-space multi-reference coupled cluster framework: An efficient and novel approach. *J. Chem. Phys. 138*, 094108-9.
(80) Nooijen, M.; Snijders, J. G. Second order many-body perturbation approximations to the coupled cluster Green's function. *J. Chem. Phys.* **1995**, *102*, 1681−1688.
(81) The CIS(D) method of Head-Gordon and co-workers is in similar spirit to a second order approximation to the EOMEE-CCSD. See ref 82.
(82) Head-Gordon, M.; Rico, R. J.; Oumi, M.; Lee, T. J. A doubles correction to electronic excited states from configuration interaction in the space of single substitutions. *Chem. Phys. Lett.* **1994**, *219*, 21−29.
(83) by using the same strategy generally used to evaluate non iterative N7 scaling three body terms in H in an iterative N5 way.
(84) N5 simplifications to EOMCCSD were presented by other groups also. Bartlett and co-workers have presented the P-EOM-MBPT(2) (ref 85) method. Krylov and co-workers have persuade the IP-CISD method (ref 30). However, rigorous benchmarking of geometry and IR frequency, with other theoretical methods and experiment, were not performed in both of the cases.
(85) Gwaltney, S. R.; Nooijen, M.; Bartlett, R. J. Simplified methods for equation-of-motion coupled-cluster excited state calculations. *Chem. Phys. Lett.* **1996**, *248*, 189−198.
(86) The advantage will not be present in the case of the EOMEA-MBPT(2) method. The EA calculation will require the ⟨ab|cd⟩ integrals and, consequently, will have the same storage requirement as that of EOMEA-CCSD. However, the EOMEA-CCSD(2) method will still have the reduced scalling of N5.
(87) Frisch, M. J.; Trucks, G. W.; Schlegel, H. B.; Scuseria, G. E.; Robb, M. A.; Cheeseman, J. R.; Scalmani, G.; Barone, V.; Mennucci, B.; Petersson, G. A.; Nakatsuji, H.; Caricato, M.; Li, X.; Hratchian, H. P.; Izmaylov, A. F.; Bloino, J.; Zheng, G.; Sonnenberg, J. L.; Hada, M.; Ehara, M.; Toyota, K.; Fukuda, R.; Hasegawa, J.; Ishida, M.; Nakajima, T.; Honda, Y.; Kitao, O.; Nakai, H.; Vreven, T.; Montgomery, J. A.; Peralta, J. E.; Ogliaro, F.; Bearpark, M.; Heyd, J. J.; Brothers, E.; Kudin, K. N.; Staroverov, V. N.; Kobayashi, R.; Normand, J.; Raghavachari, K.; Rendell, A.; Burant, J. C.; Iyengar, S. S.; Tomasi, J.; Cossi, M.; Rega, N.; Millam, J. M.; Klene, M.; Knox, J. E.; Cross, J. B.; Bakken, V.; Adamo, C.; Jaramillo, J.; Gomperts, R.; Stratmann, R. E.; Yazyev, O.; Austin, A. J.; Cammi, R.; Pomelli, C.; Ochterski, J. W.; Martin, R. L.; Morokuma, K.; Zakrzewski, V. G.; Voth, G. A.; Salvador, P.; Dannenberg, J. J.; Dapprich, S.; Daniels, A. D.; Farkas; Foresman, J. B.; Ortiz, J. V.; Cioslowski, J.; Fox, D. J. *Gaussian 09, Revision B.01*; Gaussian, Inc., Wallingford, CT, 2009.
(88) Stanton, J. F., Gauss, J., Harding, M. E.; Szalay, P. G. *CFOUR: Coupled-Cluster techniques for Computational Chemistry*. A quantum-chemical program package (with contributions from A. A. Auer, R. J. Bartlett, U. Benedikt, C. Berger, D. E. Bernholdt, Y. J. Bomble, L. Cheng, O. Christiansen, M. Heckert, O. Heun, C. Huber, T.-C. Jagau, D. Jonsson, J. Jusélius, K. Klein, W. J. Lauderdale, D. A. Matthews, T. Metzroth, L. A. Mück, D. P. O'Neill, D. R. Price, E. Prochnow, C. Puzzarini, K. Ruud, F. Schiffmann, W. Schwalbach, S. Stopkowicz, A. Tajti, J. Vázquez, F. Wang, and J. D. Watts, and the integral packages MOLECULE (J. Almlöf and P. R. Taylor), PROPS (P. R. Taylor), ABACUS (T. Helgaker, H. J. Aa. Jensen, P. Jørgensen, and J. Olsen), and ECP routines by A. V. Mitin and C. van Wüllen. (For the current version, see http://www.cfour.de.)
(89) Kendall, R. A.; Dunning, J. T. H.; Harrison, R. J. Electron affinities of the first-row atoms revisited. Systematic basis sets and wave functions. *J. Chem. Phys.* **1992**, *96*, 6796−6806.
(90) Burton, N. A.; Yamaguchi, Y.; Alberts, I. L.; Schaefer, H. F., III. Interpretation of excited state Hartree−Fock analytic derivative anomalies for NO_2 and HCO_2 using the molecular orbital Hessian. *J. Chem. Phys.* **1991**, *95*, 7466−7478.
(91) Jackels, C. F.; Davidson, E. R. The two lowest energy $^2A''$ states of NO_2. *J. Chem. Phys.* **1976**, *64*, 2908−2917.
(92) Kaldor, U. Symmetry breaking in radicals: NO_2, NS_2 and NO_3. *Chem. Phys. Lett.* **1991**, *185*, 131−135.
(93) Lafferty, W. J.; Sams, R. L. The high resolution infrared spectrum of the $2\nu_2 + \nu_3$ and $\nu_1 + \nu_2 + \nu_3$ bands of $^{14}N^{16}O_2$: Vibration and vibration-rotation constants of the electronic ground state of $^{14}N^{16}O_2$. *J. Mol. Spectrosc.* **1977**, *66*, 478−492.
(94) Morino, Y.; Tanimoto, M.; Saito, S.; Hirota, E.; Awata, R.; Tanaka, T. Microwave spectrum of nitrogen dioxide in excited vibrational states—Equilibrium structure. *J. Mol. Spectrosc.* **1983**, *98*, 331−348.
(95) Weaver, A.; Arnold, D. W.; Bradforth, S. E.; Neumark, D. M. Examination of the $^2A'_2$ and $^2E''$ states of NO_3 by ultraviolet photoelectron spectroscopy of NO^{-3}. *J. Chem. Phys.* **1991**, *94*, 1740−1751.
(96) Friedl, R. R.; Sander, S. P. Fourier transform infrared spectroscopy of the nitrate radical ν_2 and ν_3 bands: Absolute line strength measurements. *J. Phys. Chem.* **1987**, *91*, 2721−2726.
(97) Ishiwata, T.; Fujiwara, I.; Naruge, Y.; Obi, K.; Tanaka, I. Study of nitrate radical by laser-induced fluorescence. *J. Phys. Chem.* **1983**, *87*, 1349−1352.
(98) Ishiwata, T.; Tanaka, I.; Kawaguchi, K.; Hirota, E. Infrared diode laser spectroscopy of the NO_3 ν_3 band. *J. Chem. Phys.* **1985**, *82*, 2196−2205.
(99) Kawaguchi, K.; Hirota, E.; Ishiwata, T.; Tanaka, I. A reinvestigation of the NO_3 1492 cm^{-1} band. *J. Chem. Phys.* **1990**, *93*, 951−956.
(100) Davy, R. D.; Schaefer, H. F., III. Is there an absence of threefold symmetry at the equilibrium geometry of the ground electronic state for NO_3? *J. Chem. Phys.* **1989**, *91*, 4410−4411.
(101) Stanton, J. F.; Gauss, J.; Bartlett, R. J. On the choice of orbitals for symmetry breaking problems with application to NO_3. *J. Chem. Phys.* **1992**, *97*, 5554−5559.
(102) Crawford, T. D.; Stanton, J. F. Some surprising failures of Brueckner coupled cluster theory. *J. Chem. Phys.* **2000**, *112*, 7873−7879.
(103) Kaldor, U. The ground state geometry of the NO_3 radical. *Chem. Phys. Lett.* **1990**, *166*, 599−601.
(104) Eisfeld, W.; Morokuma, K. A detailed study on the symmetry breaking and its effect on the potential surface of NO_3. *J. Chem. Phys.* **2000**, *113*, 5587−5597.
(105) Eisfeld, W.; Morokuma, K. Theoretical study of the potential stability of the peroxo nitrate radical. *J. Chem. Phys.* **2003**, *119*, 4682−4688.
(106) Olson, L. P.; Kuwata, K. T.; Bartberger, M. D.; Houk, K. N. Conformation-Dependent State Selectivity in O−O Cleavage of ONOONO: An "Inorganic Cope Rearrangement" Helps Explain the Observed Negative Activation Energy in the Oxidation of Nitric Oxide by Dioxygen. *J. Am. Chem. Soc.* **2002**, *124*, 9469−9475.
(107) Bhatia, S. C.; Hall, J. H. A matrix-isolation-infrared spectroscopic study of the reactions of nitric oxide with oxygen and ozone. *J. Phys. Chem.* **1980**, *84*, 3255−3259.
(108) Dutta, A. K.; Vaval, N.; Pal, S. NOx Catalyzed Pathway of Stratospheric Ozone Depletion: A Coupled Cluster Investigation. *J. Chem. Theory Comput. 8*, 1895−1901.
(109) Morris, V. R.; Bhatia, S. C.; Hall, J. H. Ab initio self-consistent field study of the vibrational spectra for nitrate radical geometric isomers. *J. Phys. Chem.* **1990**, *94*, 7414−7418.
(110) Huber, K. P.; Herzberg, G. *Molecular Spectra and Molecular Structure. IV. Constants of Diatomic Molecules*; Van Nostrand Reinhold: New York, 1979.
(111) Piotr, A. P.; Stephen, A. A.; Stephen, E. B.; Anna, I. K.; Sherrill, C. D. Benchmark full configuration interaction and equation-of-motion

coupled-cluster model with single and double substitutions for ionized systems results for prototypical charge transfer systems: Noncovalent ionized dimers. *J. Chem. Phys.* **2007**, *127*, 164110.
(112) Pieniazek, P. A.; Bradforth, S. E.; Krylov, A. I. Charge localization and Jahn−Teller distortions in the benzene dimer cation. *J. Chem. Phys.* **2008**, *129*, 074104-11−.